Assessment of the role of green hydrogen as the commodity enabling a new green dialogue among the Mediterranean shores

Energy Conversion and Management: X 23 (2024) 100614

Contents lists available at ScienceDirect

Energy Conversion and Management: X

journal homepage: www.sciencedirect.com/journal/energy-conversion-and-management-x

Assessment of the role of green hydrogen as the commodity enabling a new green dialogue among the Mediterranean shores

A. Mazza [a,*], A. Forte [a], E. Bompard [a], G. Cavina [b], A.M. Angelini [b], M. Melani [c]

[a] EST@energycenter – Politecnico di Torino, Italy
[b] Progetti Europa & Global S.p.A. (PEG), Italy
[c] Progetti Europa & Global S.p.A. (PEG) and Link Campus University, Italy

ARTICLE INFO

Keywords:
Green hydrogen
Energy Transition
Green energy Dialogue
Plant design
Georeferenced information

ABSTRACT

The Mediterranean basin has been characterized by a net flow of fossil commodities from the North African shore to Southern Europe and the Middle East for decades; however, decarbonizing the energy system implies to substantially modify this situation, turning the current "black dialogue" into a "green dialogue" (i.e., based on the exchange of renewable electricity and green hydrogen). This paper presents a feasibility study conducted to estimate the potential green hydrogen production by electrolysis in three Tunisian sites. It shows and compares several plant layouts, varying the size and typology of renewable electricity generators and electrolyzers. The work adopts local weather data and technical features of the technologies in the computations, and accounts for site specific topographical and infrastructural constraints, such as land available for construction and local power grid connection capacities. It shows that configurations able to produce large quantities of green hydrogen may not be compliant with such constraints, basically nullifying their contribution in any hydrogen strategy. Finally, results show that the *LCOH* lies in the range 1.34 $/kg$_{H2}$ and 4.06 $/kg$_{H2}$ depending on both the location and the combination of renewable electricity generators and electrolyzers.

Introduction

In the last 30 years, global greenhouse gases (GHG) emissions have dramatically increased: despite the recent Climate Change Conferences (COP) of Sharm-El-Sheikh and Dubai reiterated the necessity of reaching the net zero commitment [1,2], the most recent emission estimations are pessimistic. In fact, in 2019 they reached around 50 Mt$_{CO2eq}$ globally, increasing by more than 50% with respect to 1990 [3]. This trend, although temporarily reduced in the following two years because of the economic consequences of the pandemic, is not sustainable and calls for a multisectoral approach involving different energy carriers to satisfy different needs. Electrification should be pursued whenever possible, even though it must account for its related carbon intensity: as shown in [4], electrification processes in Europe and Asia brought to opposite results in terms of environmental benefits, with the first generally characterized by considerably lower emission factors, mainly due to relevant mitigation policies issued by the EU [5]. Nevertheless, final energy consumption cannot be integrally electrified, because either non-convenient or non-feasible. In particular, the production of high-temperature process heat (i.e., higher than 500°C) is still scarcely electrified, both for intrinsic limitations (electricity-based heat methods are often not able to go beyond 800°C) and because the involved processes (e.g., steel, cement and glass production) cannot be quickly adapted to be electricity-fed [6–8]. These industrial processes are usually referred to as "hard-to-abate" and can represent the real driver for the development of a green hydrogen supply chain. In fact, replacing fossil fuels with hydrogen in these sectors requires less effort, with respect to a complete electricity-based process overhaul [9]; moreover, establishing a robust green-hydrogen supply chain in these industrial fields might lead to its adoption (as an energy vector) also in other sectors like mobility.

The term "green hydrogen" was used for the first time by the NREL in 1995, as a synonym of "hydrogen produced starting from renewables" [10], although there is no universally accepted definition of green hydrogen, as stated by [11]. In February 2023, the European Commission provided some key points to identify green hydrogen and the secondary commodities that can be derived from the former: first of all, hydrogen has to be synthetized via electrolysis, whose upstream electricity flow must come from renewables (some additional indications are provided for declaring electricity as such, according its related CO_2 emissions) and can be withdrawn either from the grid (with the

* Corresponding author.
E-mail address: andrea.mazza@polito.it (A. Mazza).

https://doi.org/10.1016/j.ecmx.2024.100614
Received 20 February 2024; Received in revised form 19 April 2024; Accepted 29 April 2024
Available online 6 May 2024

Nomenclature

$\mathscr{K}$ Set of RES-based plant technology under analysis
$\mathscr{I}$ Set of combinations of RES-based plant technologies and electrolysis technologies under analysis
$\mathscr{J}$ Set of combinations of RES-based plant technologies and electrolysis technologies under analysis
$\mathscr{S}$ Set of sites under analysis
$\mathbf{G}^{(s)} \in \mathbb{R}^{(H,Y)}$ Hourly irradiance matrix of the *s*–th site [W/m^2]
$\mathbf{M}_{\mathrm{H2}}^{(s,i)} \in \mathbb{R}^{(H,Y)}$ Hourly green hydrogen production in the *s*–th site [kg$_{\mathrm{H2}}$/h]
$\mathbf{P}_{\mathrm{grid}}^{(s,i)} \in \mathbb{R}^{(H,Y)}$ Hourly grid injection in the *s*–th site [kWh]
$\mathbf{P}_{\mathrm{H2}}^{(s,i)} \in \mathbb{R}^{(H,Y)}$ Hourly electricity consumption by the electrolyzer in the *s*–th site [kWh]
$\mathbf{P}_{\mathrm{RES}}^{(s,i)} \in \mathbb{R}^{(H,Y)}$ Hourly renewable electricity generation the *s*–th site [kWh]
$\boldsymbol{T}^{(s)} \in \mathbb{R}^{(H,Y)}$ Hourly air temperature matrix of the *s*–th site [°C]
$\boldsymbol{V}^{(s)} \in \mathbb{R}^{(H,Y)}$ Hourly windspeed (at a hub height of 10 m) matrix of the *s*–th site *s* [m/s]
$\boldsymbol{W}_{\mathrm{H2O}}^{(s,i)} \in \mathbb{R}^{(H,Y)}$ Hourly water consumption for green hydrogen production in the *s*–th site [kg$_{\mathrm{H2O}}$/h]
γ Oversizing factor to account for multiple electrolyzers
δ Rate of interest
ζ Conversion factor from Nm^3 to m^3 [Nm^3/m^3]
ξ Specific volume of hydrogen [Nm$^3_{\mathrm{H2}}$/kg$_{\mathrm{H_2}}$]
$\varsigma_{\mathrm{O\&M,ELY},i}$ Percentual Operation & Maintenance costs of the electrolysis plant of the *i*–th combination [%]
$\varsigma_{\mathrm{O\&M,RES},i}$ Percentual Operation & Maintenance costs of the RES plant of the *i*–th combination [%]
$\varsigma_{\mathrm{O\&M,SUB},i}$ Percentual Operation & Maintenance costs of the electrical substation of the *i*–th combination [%]
α_j Surface occupied by the *j*-th electrolyzer technology [m^2]
α_k Specific surface footprint of the *k*-th renewable electricity generation plant technology [MW/km^2]
$\mu_j^{(\mathrm{el})}$ Specific electricity consumption of the *j*-th electrolyzer technology [kWh$_{\mathrm{el}}$/kg$_{\mathrm{H2}}$]
$\mu_j^{(\mathrm{w})}$ Specific water consumption of the *j*-th electrolyzer technology [l/Nm$^3_{\mathrm{H2}}$]
$\nu^{(s)}$ Surface Roughness of the *s*-th site [-]
ϑ Size ratio between electrolyzer and RES technology [-]
$c_{\mathrm{RES},i}$ Specific costs for the RES technologies employed in the *i*-th combination in the *s*-th site [$/kg$_{\mathrm{H2}}$]
$c_{\mathrm{ELY},i}$ Specific costs for the electrolysis technologies employed in the *i*-th combination in the *s*-th site [$/kg$_{\mathrm{H2}}$]
$c_{\mathrm{W}}^{(s)}$ Specific costs of water supply in the *s*–th site [$/m^3]
$\dot{m}_j^{(\mathrm{H_2})}$ Rated hydrogen mass–flow rate of the *j*-th electrolyzer technology [kg$_{\mathrm{H2}}$/h]
$g_{k,s,t}$ Production of the generation plant (time step *t*) [MW]
$p_{j,s,t}$ Power absorbed by the electrolysis plant (time step *t*) [MW]
$p_{\mathrm{grid},t}$ Power injected into the grid (time step *t*) [MW]
$w^{(s)}$ Water availability of the *s*-th site [m^3]
N Number of electrolyzers
Y Duration of the investment [years]
$A_i^{(s)}$ Surface occupied by the *i*–th green hydrogen plant [m^2]
$A_{i,j}^{(s)}$ Surface occupied by the *i*–th electrolysis plant [m^2]
$A_{i,k}^{(s)}$ Surface occupied by the *i*–th RES plant [m^2]
$A^{(s)}$ Surface availability of the *s*-th site [m^2]
$A_{i,\,SUB}^{(s)}$ Surface footprint of the *s*–th power substation [m^2]
$C_i^{(s)}$ Total cost of the i-th combination in the *s*-th site [$]
$C_{i,\,\mathrm{CAPEX}}^{(s)}$ Total overnight capital expenditure in the *s*–th site [$]
$C_{i,\,\mathrm{OPEX}}^{(s)}$ Total overnight discounted operational expenditure in the *s*–th site [$]
$C_{\mathrm{INV,RES},i}^{(s)}$ Investment cost for the RES-based power plant of the *i*-th combination used in the *s*-th site [$]
$C_{\mathrm{INV,ELY},i}^{(s)}$ Investment cost for the electrolysis plant of the *i*-th combination used in the *s*-th site [$]
$C_{\mathrm{INV,SUB},i}^{(s)}$ Investment cost for the electrical substation of the *i*-th combination used in the *s*-th site [$]
$C_{\mathrm{L}}^{(s)}$ Cost of the land in the *s*–th site [$/ha]
$C_{\mathrm{O\&M,RES},i}^{(s)}$ Operation and maintenance costs for the RES-based power plant of the *i*-th combination used in the *s*-th site [$]
$C_{\mathrm{O\&M,ELY},i}^{(s)}$ Operation and maintenance costs for the electrolysis plant of the *i*-th combination used in the *s*-th site [$]
$C_{\mathrm{O\&M,SUb},i}^{(s)}$ Operation and maintenance costs for the electrical substation of the *i*-th combination used in the *s*-th site [$]
$C_{\mathrm{REP},i}$ Costs for the replacement of the electrolyzer stack [$]
$C_{\mathrm{REP},y}^{(i)}$ Costs for the replacement of the electrolyzer stack for the electrolysis technology of the *i*-th combination under analysis in the year *y* [$]
$C_{\mathrm{W},i,y}^{(s)}$ Costs of water supply for the *i*-th combination used in the *s*-th site in the year *y* [$]
$E_{\mathrm{RES}}^{(s,i)}$ Total renewable electricity generation in the *s*–th site, across the entire investment period [GWh]
$E_{\mathrm{RES},y}^{(s,i)}$ Yearly renewable electricity generation in the *s*–th site [GWh/y]
$E_{\mathrm{ELY}}^{(s,i)}$ Total electricity consumption of the electrolyzer in the *s*–th site, across the entire investment period [GWh]
$E_{\mathrm{ELY},y}^{(s,i)}$ Yearly electricity consumption of the electrolyzer in the *s*–th site [GWh/y]
$E_{\mathrm{grid}}^{(s,i)}$ Total electricity injected into the grid in the *s*–th site, across the entire investment period [GWh]
$E_{\mathrm{grid},y}^{(s,i)}$ Yearly electricity injected into the grid in the *s*–th site [GWh/y]
$M_{\mathrm{H2}}^{(s,i)}$ Total green hydrogen production in the *s*–th site, across the entire investment period [kt$_{\mathrm{H2}}$]
$M_{\mathrm{H2,max}}^{(s,i)}$ Maximum green hydrogen production of the *i*-th renewable electricity generation plant [kt$_{\mathrm{H2}}$]
$M_{\mathrm{H2},y}^{(s,i)}$ Yearly green hydrogen production in the *s*–th site [kt$_{\mathrm{H2}}$/y]
$V_{\mathrm{H2}}^{(s,i)}$ Total green hydrogen volume in the *s*–th site, across the entire investment period [MNm$^3_{\mathrm{H2}}$]
$V_{\mathrm{H2,y}}^{(s,i)}$ Yearly green hydrogen volume in the *s*–th site [MNm$^3_{\mathrm{H2}}$/y]
$W_{\mathrm{H2O}}^{(s,i)}$ Total water consumption in the *s*–th site, across the entire investment period [kt]
$W_{\mathrm{H2O},y}^{(s,i)}$ Yearly water consumption in the *s*–th site [kt/y]
H Number of hours per year (8760)
$M_{\mathrm{H2}}^{(\mathrm{pt})}$ Green hydrogen production target [t/y]
$\check{P}_{\mathrm{ELY},j}$ Lower operating range threshold of the *j*-th electrolyzer technology [MW]
$\widehat{P}_{\mathrm{grid}}^{(s)}$ Grid connection capacity of the *s*-th site [MVA]
P_j Rated power of the *j*-th electrolyzer [MW]
$P_{\mathrm{ELY},i}^{(s)}$ Installed capacity of the *i*-th electrolysis plant [GW]
$P_{\mathrm{RES}}^{(s,i)}$ Installed capacity of the *i*-th renewable electricity generation plant [GW]

$P^{(s,i)}_{\text{RES, max}}$	Maximum installable capacity of the i-th renewable electricity generation plant [GW]	$LCOH^{(s)}_i$	Levelized cost of hydrogen of the i-th combination in the s–th site [\$/kg$_{H2}$]

necessity to study the impact of the hydrogen plant operation on the electrical system [12] or from an ad–hoc generation plant [5]. At the end of 2020, China issued the first standard about green hydrogen, by providing two different CO_2 emission thresholds for Low-Carbon and Clean hydrogen [13]. The US Department of Energy released at the end of 2022 the standard draft on clean hydrogen production, by defining the target on well-to-gate emissions [14].

In this regard, the synthesis of green hydrogen via electrolysis may achieve lifecycle GHG emissions as low as 0.5 kg$_{CO2eq}$/kg$_{H2}$ or 1.0 kg$_{CO2eq}$/kg$_{H2}$ when adopting wind or PV generators, respectively [15].

Current framework and future perspectives for the Mediterranean basin

Among the different world regions, in this work we focus on the Mediterranean basin, because it presents peculiarities that make it a perfect real-world test ground for approaching the problem of the decarbonization of final energy uses. In fact, it includes countries at considerably diversified stages of both their actual decarbonization needs and policy-based decarbonization targets. For comparative purposes, we grouped the Mediterranean countries into three main areas that we named "shores": the Northern shore (Albania, Bosnia and Herzegovina, Croatia, France, Greece, Italy, Malta, Montenegro, Portugal, Slovenia, and Spain); the Eastern shore (Cyprus, Israel, Lebanon, Syria, and Türkiye); the Southern shore (Algeria, Egypt, Libya, Morocco, and Tunisia). The main differences among the three shores are synthetically represented in Fig. 1, where the black labels refer to the entire Mediterranean basin, while the colored boxes to the Northern, Southern and Eastern shores, respectively.

Here follow some considerations about the different aspects depicted in Fig. 1:

• *Demography*. The Mediterranean region counts an overall population of 540 million persons, equal to 6.84% of the world total, and a gross domestic product (GDP) of 9.27 \$[1], corresponding to 9.61% of the global value[2] [16,17]. The Northern shore produces 77.0% of the overall Mediterranean GDP[3], pulled by the three most economically advanced countries of the basin, namely France (GDP: 3.0 T\$), Italy (GDP: 2.1 T\$) and Spain (GDP: 1.4 T\$), the three of which alone account for 70.0% of the Mediterranean GDP. Much more modest contributions characterize the Southern (GDP: 0.76 T\$, 8.2% of the total) and the Eastern (GDP: 1.37 T\$, 14.8% of the total) shores, immediately highlighting their uneven levels of economic development, and consequently the different standards of quality of life of their citizens.

• *Geopolitical stability*. The average value of the Worldwide Governance Indicator (WGI) index, developed by World Bank [16,17], for the Mediterranean countries equals 50.49[4]. However, the Northern shore shows a WGI index of 65.28, which is more than twice that of the Southern shore (WGI: 26.87), and more than one and a half that of the Eastern one, equal to 37.47.

• *Energy needs*. The Mediterranean total primary energy supply (TPES) is equal to 41.15 EJ/y[5], which means 6.8% of the global TPES [18]: 24.42 EJ/y (59.3% of the total) supply the Northern shore only, while the remaining part is spread between the Southern (TPES: 8.82 EJ/y, 21.4% of the total), with relevant differences among its five countries, and the Eastern (TPES: 7.91 EJ/y, 19.2% of the total).

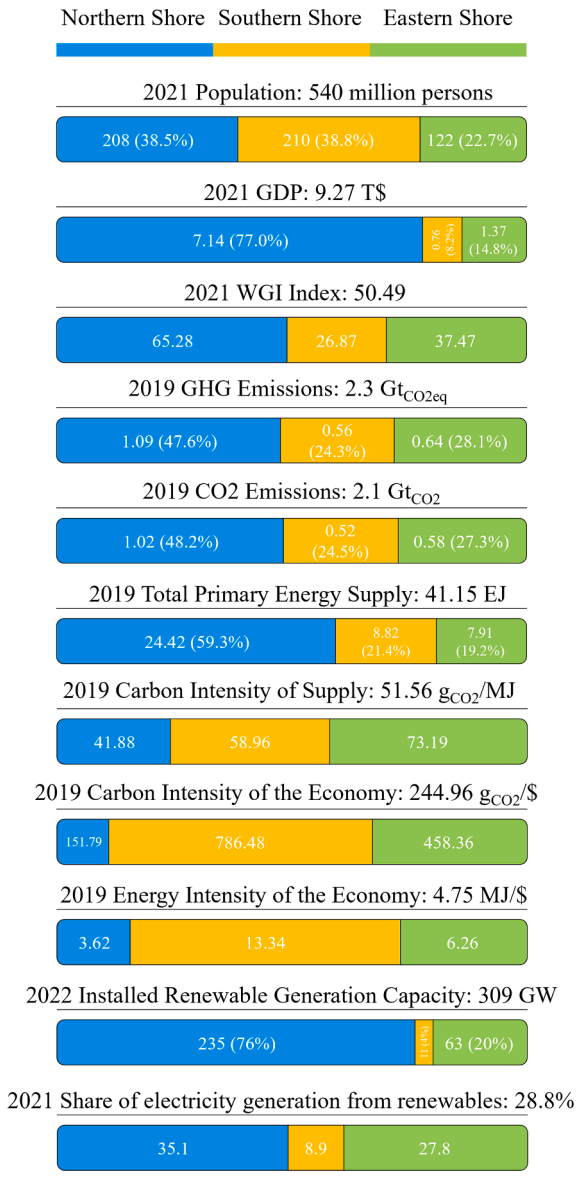

Fig. 1. Graphical characterization of the Mediterranean basin.

• *Energy mix*. In the Northern shore, 35.1%[6] of electricity generation comes from renewable energy sources, while in the Southern shore they account for only 8.9%. Even though the figure of the Eastern shore is equal to 27.8%, this value is strongly influenced by Türkiye, whose renewable sources make 35.4% of its overall electricity generation, whereas they account for no more than 10% in the other four countries [19].

• *Energy intensity*. The ratio between the GDP and the TPES is defined as energy intensity, and it helps assessing the energy efficiency of a system, being the energy required to produce one unit of GDP. The Northern shore ranks first with 3.62 MJ/\$, about half of the energy

[1] Current USD.
[2] 2021 data.
[3] 2021 data.
[4] 2022 data.
[5] 2019 data.
[6] 2021 data.

intensity of the Eastern shore (6.26 MJ/$), and less than 30% the energy intensity of the Southern shore, 13.34 MJ/$.

• *CO_2 emissions*. Disparities characterize the three shores also in terms of overall CO_2 emissions [3]: in this case, the Northern shore emits most of the CO_2, being responsible for 1.01 Gt_{CO2}/y out of 2.1 Gt_{CO2}/y (48.2% of the overall CO_2emissions). The remaining part is almost equally allocated to the other two shores. However, lower emissions might be evidence of the modest energy consumptions of the Southern and Eastern shores, rather than of sustainable energy systems. In fact, by considering the carbon intensities, the Northern shore shows a carbon intensity of supply of 41.88 g_{CO2}/MJ and a carbon intensity of the economy of 151.79 g_{CO2}/$, compared against 58.96 g_{CO2}/MJ and 786.48 g_{CO2}/$ in the Southern shore and 73.19 g_{CO2}/MJ and 458.36 g_{CO2}/$ in the Eastern shore. To face this issue, in [20] the author identified strategies, pros and cons of taking up hydrogen in the industrial sector in Middle Eastern and North African countries: wind power and off–grid photovoltaic were identified as the most cost-effective and easily implementable technologies for the effective development of a hydrogen generation and distribution infrastructure.

• *Natural resources*. The quasi-totality of the Mediterranean gas and oil reserves is located in the countries of the Southern shore, which hold 94.9% of their total amount (natural gas: 206.5 Tm^3 out of 217.5 Tm^3, oil: 7.89 Mt out of 8.31 Mt). In terms of coal reserves though, none are located in the Southern shore, whereas 73.9% (11.5 Gt out of 15.6 Gt) are in Türkiye only. The remaining portion is split between Greece (2.9 Gt, 18.5% of total) and Spain (1.2 Gt, 7.6% of total) [21].

In the past, all these aspects were responsible for a net energy flow from the Southern to the other two shores, and the Northern in particolar [22,23]: as examples, in 2019 Spain and Italy respectively imported 12 Gm^3/y and 19.5 Gm^3/y of natural gas from the Southern shore, corresponding to approximately 33% and 27% of their respective total imports. Such figures have since increased because of the reduction of Russian gas imports that followed the outbreak of the Russo–Ukranian crisis*:* in 2023, Spanish gas imports from the Southern shore amounted to 11.4 Gm^3/y,(30.3% of total imports) while Italian ones to 28.2 Gm^3/y, accounting for 47.1% of the total imports [24–26]. The export of natural gas, crude oil and petroleum products to the Northern shore actually is one of the major sources of income for both Algeria and Libya [27], considering that it was worth 13.7 B$ for the first and 10.9 B$ for the second, respectively representing 94.4% and 99.1% of their overall economic value of exports, and 8.0% and 15.7% of their GDP. This kind of *black dialogue* cannot be kept in the medium-long term, due to the decarbonization targets to be accomplished by the countries of the Northern shore: as stated in the EU 2050 long-term strategy [28] and later by the European Parliament in 2020 in the EU Green deal [29], Europe is committed to reach a net-zero greenhouse gas emission economy[7]. A new green dialogue, based on the exchange of green sources and carriers, must actively engage all the shores and share all its potential benefits as much as possible. The Southern shore can play a major role in this transition, because it presents the most promising solar and wind potentials, with an average global horizontal irradiance of 5.67 kWh/m^2 [31] and an average wind speed[8] of 8.76 m/s [32]. As a matter of comparison, the Eastern shore shows an average horizontal irradiance of 5.12 kWh/m^2, while the Northern one only 4.02 kWh/m^2 [31]; the same situation can be observed in terms of wind speed, with an average of 7.67 m/s and 7.11 m/s in the Northern and Eastern shores, respectively [32]. In spite of the considerable higher renewable potential, the PV installed capacity in the Southern shore only amounts to 2.4 GW (57.1 GW in the Northern shore, 10.5 GW in the Southern shore [33], and the onshore wind to 3.3 GW (68.4 GW in the Northern shore).

[7] Even though the entire Europe accounts for less than 8% of the total worldwide CO_2 emissions, and less than about 6% of the total worldwide GHG emission [30].

[8] At a height of 100 m.

[34] and [35] showed the pivotal role of RES in the uptake of green hydrogen, but at the same time stated that renewables only cannot pave the way to the decarbonization of the current energy system, because of significant technological and geopolitical implications. The more than considerable bilateral political and societal effort between Europe and North Africa is further underlined in [36].

The integration of green hydrogen into the existing energy system of the Mediterranean basin is supported by national and supranational regulatory and policy frameworks. At the EU level, not only member countries are pursuing the objective set by the European Commission to deploy an overall 40 GW electrolyzer capacity by 2030, but the EU itself is planning to install 40 GW of further capacity in neighboring countries with the aim of importing additional volumes of green hydrogen from abroad [37]. Additionally, EU member countries of the Northern shore (with the only exception of Malta) included hydrogen in their 2030 energy mix and provided key figures in either their respective National Climate and Energy Plans (NECPs) or in their national hydrogen strategies.

Slovenia did not explicitly state any electrolysis capacity to be deployed; however, it foresees the deployment of two electrolysis units devoted to store excess electricity in the form of hydrogen for subsequent use.

The recap of electrolysis capacity penetration targets are displayed in Table 1.

In the Southern Shore, Morocco launched its hydrogen strategy aiming at installing 2.8 GW of electrolyzers within 2030 [45]. The same did Algeria and Tunisia, targeting approximately 200 MW and 3.85 GW of electrolysis capacity, respectively [46,47]. Egypt plans to become a major player in the future hydrogen market, pursuing global market shares as high as 5% to 8% [48].

In the Eastern shore, Israel is foreseeing a significant integration of hydrogen in the energy mix by 2050: by that time, the country forecasts to deploy from 2.9 GW to 8.0 GW of electrolyzers. In Türkiye, the government is intentioned to deploy 2 GW of electrolyzers by 2030, 5 GW by 2035, and a remarkable capacity of 70 GW by 2053 [49].

The relatively recent and widespread diffusion of green hydrogen–related targets hints at how most of the Mediterranean countries not only are keen on adopting hydrogen as an energy commodity in their near–future energy mixes but are also consequently committed to develop an ad–hoc regulatory framework to speed up its uptake in the next years.

Moreover, the European Hydrogen Backbone project already envisages the exploitation of the Transmed, Medgaz and TAP gas pipeline to transport gas–hydrogen blends, so to build a hydrogen–based dialogue among the three shores in the near–future [50].

Literature overview

The creation of adequate green hydrogen infrastructures that actively involve the Southern shore as part of a Mediterranean basin decarbonization process requires: i) the evaluation of the RES potential, ii) the design of the green hydrogen production plants and iii) the transport towards the other shores exploiting, if possible, the existing gas transport infrastructure. Several authors have investigated the problem in recent years.

Table 1
2030 electrolyzer installation targets for EU countries of the Northern shore.

Country	Electrolyzer capacity target [GW]	Source
Croatia	0.07	[38]
France	6.5	[39]
Greece	0.8	[40]
Italy	5.0	[41]
Portugal	5.5	[42]
Slovenia	Not specified	[43]
Spain	11.0	[44]

Recently, [51] used the topology and the main physical characteristics of the European, Middle Eastern and North African transmission grid (as available from ENTSO-E) to feed the ATLANTIS energy optimization model, with the aim of computing the renewable electricity production potential along the two shores until 2030. Other authors implemented bottom-up approaches to compute green hydrogen production starting from site-specific climate data, used in turn to evaluate the producibility of PV and onshore wind power plants [52,53].

The problem of finding the cost–optimal solution was studied by various literature contributions, implementing either electrolysis or other carbon–free synthesis methods. The energy system optimization model HOMER was employed to find the cost-optimal PV– and/or wind–based generation mix in different locations in Canada, USA and Australia in [54]), and in five Saudi Arabian cities in [55]; in [56] HOMER was adopted to find the least–cost option in a green hydrogen–green methanol plant starting from local weather data. Weather data itself was used by [57] and [58]; the first computed electricity production from a PV plant, and then ran a Monte Carlo–based optimization model to find the PV–electrolyzer combination with the lowest Levelized Cost Of Hydrogen (*LCOH*); the second implemented genetic algorithms to find the cost-optimal configuration between offshore wind farms, storage and electrolysis systems. [59] and [60] also used weather information to compare several renewable–electrolysis combinations for Morocco.

In [61], the authors assessed the possibility of producing green hydrogen in a run-of-river power plant: green hydrogen mass-flow rate was computed from real–time power generation, and the electrolyzer chosen selecting the size which returned the best tradeoff between efficiency and hydrogen production.

Other authors adopted an inverse, top–down approach, in which the size of either the renewable electricity or the electrolysis plant was inferred and computed starting from a known value of hydrogen demand. In [62] annual solar irradiance values of several Algerian sites were used to model the electricity production from a solar tower and size the electrolyzer starting from a target value of hydrogen mass-flow rate. In [63] the authors designed the electrolysis plant to be installed in a hydrogen valley in Italy, starting from mass–flow rate data provided by industrial partners and coupling it to solar irradiance data. Green hydrogen production from biogas was estimated in [64] starting from known process values of a biogas production plant.

Some authors also investigated the problem of transporting green hydrogen–gas blends. [65] assessed the potential of blending green hydrogen into the Italian natural gas network as a tool for policy makers, claiming that Italy could also give at least a 1% contribution to the EU hydrogen strategy [37] by deploying plants for green hydrogen blending. In [66,67] the authors modelled the transport of green hydrogen–gas blends to Italy through the Greenstream pipeline: they estimated the green hydrogen demand from that of natural gas, and consequently sized a PV power plant, feeding the model input data about solar irradiance. An analogous approach was adopted in [68] to evalaute the green hydrogen production potential and its subsequent diffusion in the Algerian road transport sector. In [66,67], typical photovoltaic production curves from the PVGIS database were fed to a PV producibility model and coupled with detailed information about electricity and gas infrastructures to compute the amount of green hydrogen produced and subsequently injected into the gas network, in case of surplus RES generation. [69] started from hourly values of solar irradiance and windspeed and computed the *LCOH* of different options to produce green hydrogen in North Africa and consequently transport it in gas blends into existing European gas pipelines. Clean water for electrolysis was assumed to be produced by means of seawater desalination. The latter was suggested also in [70] as a promising technology to overcome the problem of the scarcity of clean water in North African countries and favor the development of a green hydrogen–based trade between the North African and the European shores to replace the current, fossil–based one.

Contributions of this paper

For tangibly contributing to establishing this new green dialogue, this paper presents a feasibility analysis to assess the green hydrogen production potential in Tunisia, considering three different sites. The produced hydrogen could be transported in Italy in blended form with natural gas through the Transmed pipeline. We computed the *LCOH* for different combinations of both size and technology of renewable electricity generators, and for alternative electrolyzer technologies.

The methodological approach proposed in this paper stands out as it integrates site–specific meteorological data for the computation of the power producibility profiles of renewable power plants with detailed topographical information and the infrastructural constraints imposed by the current Tunisian power distribution grid. In this framework, cost-effective solutions might be discarded because not constraint–compliant. This contribution aims to provide meaningful insights for future investments in the Southern shore countries, by highlighting issues and solutions that may be adapted in different contexts.

The rest of the paper is composed as follows: Section 2 describes the methodological approach specifically followed in this study; Section 3 illustrates the characteristics of the three sites and displays the main numerical parameters adopted for the computation of the assessed case studies; Section 4 shows the numerical results of the analysis and provides a discussion on how the penetration of green hydrogen complies and/or clashes with the current and future Tunisian energy framework; Section 5 contains the final concluding remarks of the paper.

Methodological and computational approach

The examples found in literature diffusely implemented local weather data as a starting point to assess green hydrogen production, but generally lacked a detailed infrastructural and morphological characterization of the green hydrogen production sites. On the contrary, the feasibility study presented here integrates a topographical site characterization that included, for example, the local surface roughness and altitude, and set constraints that may or may not have inhibited the selection of a potentially promising RES–electrolyzer combination. These were identified in the local water[9] and surface availabilities, and in the local power transmission connection capacity.

Fig. 2 shows the functional scheme describing the methodological approach adopted in this paper.

The process is structured into three main groups, highlighted with different colors in Fig. 2. The main goal of the procedure is to obtain the evaluation of the *LCOH*, expressed in ($/kg$_{H2}$), of different combinations of RES-based power plants and electrolysis plant by considering an investment period composed of Y years composed of H hours and taking into account as hard constraints *i*) the site available area and *ii*) the available grid connection capacity.

The procedure is composed of the following conceptual steps:

- *Step 1: definition of the hydrogen production target.* Real-world project starts from a well-established production target, namely $M_{H2}^{(pt)}$.
- *Step 2: site characterization.* Every site $s \in \mathscr{S}$ is characterized by the following information: *i*) the primary energy source (i.e., the hourly irradiance matrix $\mathbf{G}^{(s)} = \left\{g_{h,y}, h = 1, \cdots, H, y = 1, \cdots, Y\right\} \in \mathbb{R}^{(H,Y)}$, the hourly air temperature matrix $\mathbf{T}^{(s)} = \left\{t_{h,y}, h = 1, \cdots, H, y = 1, \cdots, Y\right\} \in \mathbb{R}^{(H,Y)}$ and the hourly wind speed matrix $\mathbf{V}^{(s)} =$

[9] According to onsite surveys conducted by Progetti Europa & Global S.p.A. (PEG), local freshwater resources in the three assessed sites are large enough to meet the $M_{H2}^{(pt)}$ production target. However, scaling up the electrolysis capacity could dramatically increase the pressure on the Tunisian water system. To overcome the issue, the Tunisian government announced that freshwater for electrolysis will be provided by means of seawater desalination.

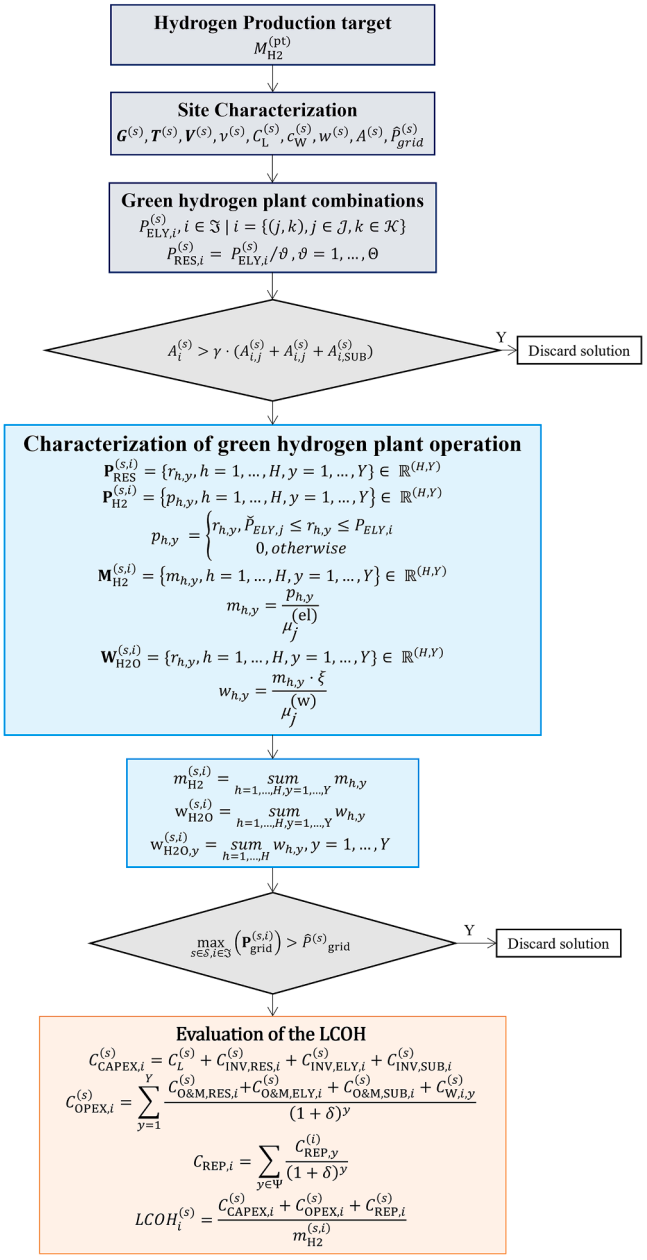

Fig. 2. Functional scheme of the methodological approach adopted in this paper.

$\{v_{h,y}, h = 1, \cdots, H, y = 1, \cdots, Y\} \in \mathbb{R}^{(H,Y)}$); *ii*) the available area $A^{(s)} \in \mathbb{R}$; *iii*) the grid connection capacity $\hat{P}_{grid}^{(s)}$; the topographical characterization (i.e., the surface roughness $v^{(s)}$, and the water resources $w^{(s)}$). The topographic and weather information was extracted from the web–integrated platform RES–Plat, developed by the Energy Security and Transition Lab (EST Lab) at Politecnico di Torino [71].

• *Step 3: definition of the green hydrogen plant combinations.* We can investigate several combinations of RES technologies $k \in \mathcal{K}$ and electrolysis technologies $j \in \mathcal{J}$, each one with different rated power $P_{RES,i}^{(s)}$ (for RES-based power plant) and $P_{ELY,i}^{(s)}$ (for electrolysis plant), respectively; for sake of simplicity and without loss of generality, we indicate each combination under analysis with the symbol $i \in \Im$, with $i = \{(j,k), \text{ with } j \in \mathcal{J}, k \in \mathcal{K}\}$. The definition of the sizes of the two plant portions were created by introducing a *sensitivity analysis*: starting from the size of the electrolysis (kept constant for all the combinations, i.e., $P_{ELY,i}^{(s)} = P_{ELY,i+1}^{(s)}, \forall i \in \Im$) the size of the RES-based power plants was obtained as $P_{RES,i}^{(s)} = P_{ELY,i}^{(s)}/\vartheta$, with $\vartheta = 1, \cdots, \Theta$ the size ratios between the electrolysis plant and the RES-based power plant.

• *Step 4: check on the surface constraint.* The first feasibility check is carried out to verify if the overall size of the *i*-th combination matches the surface availability constraint of the site. The surface occupied ($A_i^{(s)}$) is proportional to the sum of the areas covered by the electrolysis plant ($A_{i,j}^{(s)}$), the RES plant ($A_{i,k}^{(s)}$), and the electrical substation ($A_{i,SUB}^{(s)}$), i.e.:

$$A_i^{(s)} = \gamma \cdot \left(A_{i,j}^{(s)} + A_{i,k}^{(s)} + A_{i,SUB}^{(s)}\right) \quad (1)$$

The evaluation of $A_i^{(s)}$ includes an oversizing factor $\gamma = 1.2$ to account for some additional space required to install multiple electrolyzers (i.e., for enabling the establishment of paths between among the containers). If $A_i^{(s)}$ is not compatible with the available surface in the *s*–th site, the *i*-th combination is discarded.

• *Step 5: characterization of the green hydrogen plant operation.* In the case of acceptable solutions, we computed the hourly renewable power generation matrix $\mathbf{P}_{RES}^{(s,i)} = \{r_{h,y}, h = 1, \cdots, H, y = 1, \cdots, Y\} \in \mathbb{R}^{(H,Y)}$ according to technology–specific computational models fed by site-specific weather and topographic data defined in *Step 2*. On the basis of the value of RES production, it is possible to evaluate the matrices $\mathbf{P}_{H2}^{(s,i)} = \{p_{h,y}, h = 1, \cdots, H, y = 1, \cdots, Y\} \in \mathbb{R}^{(H,Y)}$, $\mathbf{M}_{H2}^{(s,i)} = \{m_{h,y}, h = 1, \cdots, H, y = 1, \cdots, Y\} \in \mathbb{R}^{(H,Y)}$ and $\mathbf{W}_{H2O}^{(s,i)} = \{w_{h,y}, h = 1, \cdots, H, y = 1, \cdots, Y\} \in \mathbb{R}^{(H,Y)}$, containing the power supplied to the electrolyzer for the green hydrogen production (in MW), the mass of the produced green hydrogen (in kg) and the corresponding volume of consumed water (in m^3). Their elements are computed as follows:

$$p_{h,y} = \begin{cases} r_{h,y}, \check{P}_{ELY,j} \le r_{h,y} \le P_{ELY,i} \\ 0, \text{ otherwise} \end{cases} \quad (2)$$

$$m_{h,y} = \frac{p_{h,y}}{\mu_j^{(el)}} \quad (3)$$

$$w_{h,y} = \frac{m_{h,y} \cdot \xi}{\mu_j^{(w)}} \quad (4)$$

with: $\check{P}_{ELY,j}$ being the lower operating range threshold of the *j*-th electrolyzer technology; $P_{ELY,i}$ is the rated power of the electrolysis plant in the *i*-th combination under analysis; $\mu_j^{(el)}$ the specific electricity consumption of the *j*-th electrolyzer technology [kWh_{el}/kg_{H2}]; ξ the specific volume of hydrogen [Nm^3_{H2}/kg_{H2}]; and $\mu_j^{(w)}$ the specific water consumption of the *j*-th electrolyzer technology [l/Nm^3_{H2}]. The total production of hydrogen can be calculated summing the elements of the matrix $\mathbf{M}_{H2}^{(s,i)}$, i.e., $m_{H2}^{(s,i)} = \underset{h=1,\cdots H,y=1,\cdots,Y}{sum} m_{h,y}$. Similarly, the total volume of water can be obtained starting from the matrix $\mathbf{W}_{H2O}^{(s,i)}$ as $w_{H2O}^{(s,i)} = \underset{h=1,\cdots,H,y=1,\cdots,Y}{sum} w_{h,y}$; the yearly water consumption, instead, may be calculated as $w_{H2O,y}^{(s,i)} = \underset{h=1,\cdots,H}{sum} w_{h,y}$, for $y = 1, \cdots, Y$.

• *Step 6: check on the grid connection constraint.* Since part of the RES-based power plants production may be not used by the electrolysis plant, we define the matrix $\mathbf{P}_{grid}^{(s,i)} = \mathbf{P}_{RES}^{(s,i)} - \mathbf{P}_{H2}^{(s,i)}$: in case $\max_{s \in \mathcal{J}, i \in \Im} (\mathbf{P}_{grid}^{(s,i)}) > \hat{P}_{grid}^{(s)}$, i.e., the excess of production overcomes the grid limit of the site *s*, the *i*-th combination is discarded.

• *Step 7: evaluation of the* $LCOH_i^{(s)}$. The $LCOH_i^{(s)}$ referring to the subset of feasible solutions was computed as follows:

$$LCOH_i^{(s)} = \frac{C_i^{(s)}}{m_{\mathrm{H2}}^{(s,i)}} \tag{5}$$

with $C_i^{(s)}$ indicating the total cost of the i-th combination in the s-th site.

The total cost $C_i^{(s)}$ is the sum of the CAPEX $C_{\mathrm{CAPEX},i}^{(s)}$ (considered overnight) and the discounted OPEX $C_{\mathrm{OPEX},i}^{(s)}$, i.e.:

$$C_{\mathrm{CAPEX},i}^{(s)} = C_{\mathrm{L}}^{(s)} + C_{\mathrm{INV,RES},i}^{(s)} + C_{\mathrm{INV,ELY},i}^{(s)} + C_{\mathrm{INV,SUB},i}^{(s)} \tag{6}$$

$$C_{\mathrm{OPEX},i}^{(s)} = \sum_{y=1}^{Y} \frac{C_{\mathrm{O\&M,RES},i}^{(s)} + C_{\mathrm{O\&M,ELY},i}^{(s)} + C_{\mathrm{O\&M,SUB},i}^{(s)} + C_{\mathrm{W},i,y}^{(s)}}{(1+\delta)^y} \tag{7}$$

with: $C_{\mathrm{L}}^{(s)}$ cost of the land belonging to the s-th site; $C_{\mathrm{INV,RES},i}^{(s)}$ and $C_{\mathrm{O\&M,RES},i}^{(s)}$ investment and Operation & Maintenance (O&M) costs for the RES-based power plant of the i-th combination used in the s-th site, respectively; $C_{\mathrm{INV,ELY},i}^{(s)}$ and $C_{\mathrm{O\&M,ELY},i}^{(s)}$ investment and O&M costs for the electrolysis plant of the i-th combination used in the s-th site, respectively; $C_{\mathrm{INV,SUB},i}^{(s)}$ and $C_{\mathrm{O\&M,SUB},i}^{(s)}$ cost of investment and O&M for the electrical substation required used in the s-th site; $C_{\mathrm{W},i,y}^{(s)}$ cost of the water for the i-th combination used in the s-th site in the year y; and δ is the discount rate. It is worth noting that the O&M costs are supposed being constant over the years.

The investment costs for the RES-based power plant and the electrolysis plant are calculated as:

$$C_{\mathrm{INV,RES},i}^{(s)} = c_{\mathrm{RES},i} \cdot P_{\mathrm{RES},i}^{(s)} \tag{8}$$

$$C_{\mathrm{INV,ELY},i}^{(s)} = c_{\mathrm{ELY},i} \cdot P_{\mathrm{ELY},i}^{(s)} \tag{9}$$

where $c_{\mathrm{RES},i}$ and $c_{\mathrm{ELY},i}$ are the specific costs (in \$/kW) for the RES and electrolysis technologies employed in the i-th combination used in the s-th site, respectively.

With reference to the yearly water cost, it can be calculated as:

$$C_{\mathrm{W},i,y}^{(s)} = c_{\mathrm{W}}^{(s)} \cdot w_{\mathrm{H2O},y}^{(s,i)} \tag{10}$$

where $c_{\mathrm{W}}^{(s)}$ represents the specific cost of the water (in \$/m^3), supposed constant for the entire investment period (i.e., it has been considered the existence of long-term contract to ensure it).

The O&M costs are supposed to be a percentage of the investment costs:

$$C_{\mathrm{O\&M,RES},i}^{(s)} = \zeta_{\mathrm{O\&M,RES},i} \cdot C_{\mathrm{INV,RES},i}^{(s)} \tag{11}$$

$$C_{\mathrm{O\&M,ELY},i}^{(s)} = \zeta_{\mathrm{O\&M,ELY},i} \cdot C_{\mathrm{INV,ELY},i}^{(s)} \tag{12}$$

$$C_{\mathrm{O\&M,SUB},i}^{(s)} = \zeta_{\mathrm{O\&M,SUB},i} \cdot C_{\mathrm{INV,SUB},i}^{(s)} \tag{13}$$

Moreover, over the investment period, it is necessary to replace the stack of the electrolyzer; hence, it is possible to introduce the set Ψ, including all the years in which a replacement is excepted and add a further cost component $C_{\mathrm{REP},i}$:

$$C_{\mathrm{REP},i} = \sum_{y \in \Psi} \frac{C_{\mathrm{REP},y}^{(i)}}{(1+\delta)^y} \tag{14}$$

where $C_{\mathrm{REP},y}^{(i)}$ represents the replacement cost for the electrolysis technology of the i-th combination under analysis in the year y.

The proposed paper stands out as the case study described herein not only relies on site–specific weather data for the computation of the renewable electricity producibility profiles, but develops a method for the feasibility study of an electrolysis plant that is tightly linked to the topographical characterization of the locations in terms of their water resources and land availability, as well as to the current state of the electricity grid, accounting for the actual capacity of the power transmission network.

The following section delineates the characteristics of the three sites, the operational design parameters of the RES generators and the electrolyzers, and the numerical values adopted for the computation of the *LCOH*.

Table 2
Morphological and infrastructural characteristics of the assessed sites.

Parameter	Site 1	Site 2	Site 3
$A^{(s)}$	$1.41 \cdot 10^6$ m^2	$3.41 \cdot 10^6$ m^2	$3.32 \cdot 10^6$ m^2
$\widehat{P}_{\mathrm{grid}}^{(s)}$	<10 MVA (@90 kV)	≈100 MVA (@225 kV)	≈100 MVA (@150 kV)
Average specific PV power output	1591 kWh/kW$_p$	1651 kWh/kW$_p$	1793 kWh/kW$_p$
Average wind speed at 10 m	5.49 m/s	2.78 m/s	2.83 m/s
Distance from the electrical infrastructure	≤10 km	≤25 km	≤20 km
Distance from the gas infrastructure	≤20 km	≤5 km	≤5 km
Water availability	>100 kt/y	>100 kt/y	>100 kt/y

Information about the case studies site characteristics

Table 2[10] recaps the main features of the three selected sites whose names, for confidentiality reasons, cannot be disclosed.

Since the promising solar and wind potentials, we considered both photovoltaic PV and onshore wind as RES generators. For every site, we assessed the electricity that may be produced from RES and the share that can be converted into hydrogen, in compliance with the constraints related to both land use and occupancy, and to the connection to the electricity grid.

Technical features of the plant components and technological combinations

RES generation

We considered crystalline silicon solar panels, as they are the most employed technology for the construction of PV modules [72], and two different mounting configurations:

- conventional, fixed structure with preset inclination and specific surface footprint $\alpha_{\mathrm{f}} = 100$ MW/km^2
- single axis sun-tracking systems, with dynamically variable azimuthal angle and surface footprint $\alpha_{1\mathrm{a}} = 66$ MW/km^2 [73].

Table 3 illustrates the main technical features of the wind generator (WG) model.

Electrolyzers

We considered two different electrolyzers, whose specifications are displayed in Table 4[11].

Electrical connection to the main grid

Power generation plants must include a HV/MV,[12] together with a usual MV/LV substation hosting the MV/LV transformer(s) and the

[10] Confidential figures disclosed to the authors by Progetti Europa & Global S. p.A. (PEG), except from solar irradiance [31] and wind speed [32].

[11] It is worth noting that the information shown in Table 4 refers to commercial electrolyzers. For additional information, please refer to [74] for the PEM technology and [75] for the alkaline technology.

[12] The area of the HV/MV substation was not included as part of the plant area, considering the possibility that it could be convenient to make an agreement with the local TSO and exploit the area of an already existing HV/MV substation, by participating to the expenses required for enhancing the HV/MV equipment (which has been included in the *LCOH* calculation).

Table 3
Main technical features of the wind turbine adopted as reference.

Rated Power	4 MW
Cut-in speed	3 m/s
Cut-out speed	~23 m/s
Wind class	IEC IIIb
Blade length	~74 m

Table 4
Main technical features of the electrolyzers.

Technical characteristics	Proton Exchange Membrane (PEM)	Alkaline
Rated electrical power [MW]	2.5	2.5
Rated hydrogen production [Nm^3/h]	500	485
H_2 delivery pressure [bar]	30	1–200
H_2 purity [%]	99.998%	99.9%
Operating range [%]	5–100%	15–100%
System Specific consumption [kWh/kg_{H2}]	≤ 54	55[13]
Freshwater consumption [l/kg_{H2} (l/Nm^3_{H2})]	17 l/kg_{H2} (1.5)	17 l/kg_{H2} (1.5)[14]
Installation environment[15]	−20 °C/40 °C, outdoor	5 °C/35 °C
Total land occupancy [m^2]	~198 m^2	~225 m^2

[13] Due to lack of information, the system consumption has been obtained starting from specific consumption of the stack (equal to 49 kWh/kg_{H2}) by adding of 6 kWh/kg_{H2} (as for PEM technology as stated in [74]).
[14] Due to lack of information the water consumption was supposed to be equal to the one of the HyLYZER 500.
[15] Considering the temperature conditions of the selected sites, one critical aspect might be the maximum admissible environmental temperature during their operation, which lies in the range 35 °C – 40 °C.

protection equipment, positioned in the assessed area. We assumed the MV/LV substation to be 15 m wide and 5 m long: these dimensions overestimate the actual dimensions of a MV/LV substation (see for example [76]), to account in advance for different plant design approaches, which can be necessary to reserve a large enough area for equipment logistics, to keep safety distances and to allow the project director to choose the best plant layout: for example, the presence of multiple transformers, additional equipment to operate separately the two plant subsystem (i.e., RES-base power plant and electrolyzer), additional measurement system for providing ancillary services to the grid, etc.

Technological combinations considered in the case studies

The following case studies considered four different combinations with a PV generator, i.e.:

- $i = 1$: PV fixed + PEM electrolyzer.
- $i = 2$: PV fixed + Alkaline electrolyzer.
- $i = 3$: one-axis tracker + PEM electrolyzer.
- $i = 4$: one-axis tracker + Alkaline electrolyzer.

Two additional combinations involving WGs were considered for site 1:

- $i = 5$: WG + PEM electrolyzer.
- $i = 6$: WG + Alkaline electrolyzer.

For matter of clearness, the results will be presented explicitly referring to the considered technologies, without enumerating the combination.

Techno–economic parameters adopted for the computation of the LCOH

The total duration of the investment is considered equal to $Y = 20$ years, while we assumed a discount rate equal to $\delta = 8\%$.

Table 5 shows the values of the techno–economic parameters adopted for the computation of the *LCOH* in each of the three sites (capital investment and operation and maintenance costs are expressed as a min–max range).

The following section presents the results obtained in the three sites, for the technology combinations listed in Section 3.2.4. We first display the main figures related to green hydrogen production along the entire duration of the investment, and then their respective values of *LCOH*. We also integrate an additional analysis showing how green hydrogen production would change, if one installed a PV generation capacity equal to the maximum allowable by the surface availability constraint.

Results and discussion

PV-fed plant − with constraints

This section shows the numerical results related to the green hydrogen production and its related *LCOH* in the three considered Tunisian sites, obtained taking into account the physical constraints imposed by both the maximum available surface, and the maximum power transmission capacity of the local grid. As anticipated in Section 2, we carried out a sensitivity analysis, in which we set the size of the electrolysis plant to $P^{(s)}_{\mathrm{ELY},i} = 100\ MW$, and defined that of the RES-based power plants as $P^{(s)}_{\mathrm{RES},i} = P^{(s)}_{\mathrm{ELY},i}/\vartheta$, being $\vartheta = 1, \cdots, \Theta$ the size ratios between the electrolysis plant and the RES-based power plant. In particular, ϑ ranges from 0.5 to 1, with a step of 0.1.

Table 6, Table 7, and Table 8 present the results of the sensitivity analysis for the three sites, for the considered period of investment. We highlighted in different colors the combinations for which either one of the constraints or both are not met, while in green those that match the yearly target hydrogen production. According to the information provided by the commissioning company, in site 1 there is not any physical electrical infrastructure yet, hence we assumed a maximum electricity transmission capacity equal to the lower operating ranges of the two electrolyzer technologies.

Site 1 is the only where almost every RES–electrolyzer combination does not fit the surface and/or transmission capacity requirements, mainly because of the very limited available surface.

In site 2, in the case of a fixed PV plant, a capacity of 200 MW is required to meet the yearly green hydrogen production target of 5 kt_{H2}/y, regardless the electrolyzer technology. In the case of 1–axis tracker PV plant, a lower capacity is necessary, thanks to the opportunity of better harnessing the incident solar radiation: in fact, it only takes a 143 MW large PV plant, equivalently an alkaline or PEM electrolyzers. Site 3, despite being slightly smaller than site 2, benefits a from an increased solar irradiance, hence enables to meet the green hydrogen production target with a smaller PV plant in three out of four cases: with PEM electrolyzers, the minimum RES capacity decreases to 167 MW in the case of a PV–fixed RES plant, and to 125 MW with a 1–axis tracker plant. With alkaline electrolyzers, the minimum RES capacity decreases to 125 MW, but only provided that 1–axis trackers are installed.

In Section 1.2 we stated that green hydrogen produced from the electrolysis plants located in the three assessed Tunisian sites would be exported to Italy, blending it with natural gas in the Transmed pipeline. To this purpose, it is worth reminding that the transport of hydrogen–gas blends into existing natural gas pipelines may require from slight to consistent repurposing interventions, depending on the amount of hydrogen that is blended. However, when the hydrogen volume fraction in the mixture is lower than 10%, no adjustments may be needed at all [85]. Referring to the 2022 total throughput of the Transmed pipeline, equal to 23.7 GSm^3/y, the hydrogen volume that could be transported

Table 5
Techno-economic parameters included in the evaluation of *LCOH*.

	Parameter		Value–Site 1	Value–Site 2	Value–Site 3	Source
Onshore wind turbine	$C^{(s)}_{INV,RES,i}$	[$/kW]	800–1350	800–1350	800–1350	[77]
	$\varsigma_{O\&M,RES,i}$	[%CAPEX/y]	0.20	0.20	0.20	[77]
	$C^{(s)}_{O\&M,RES,i}$	[$/kW]	160–1080	160–1080	160–1080	
Fixed PV plant	$C^{(s)}_{INV,RES,i}$	[$/kW]	340–834	340–834	340–834	[78]
	$\varsigma_{O\&M,RES,i}$	[%]	0.01	0.01	0.01	[78]
	$C^{(s)}_{O\&M,RES,i}$	[$/kW]	3.4–8.34	3.4–8.34	3.4–8.34	
1–axis PV plant	$C^{(s)}_{INV,RES,i}$	[$/kW]	442–1084	442–1084	442–1084	[79]
	$\varsigma_{O\&M,RES,i}$	[%CAPEX/y]	0.02	0.02	0.02	[79]
	$C^{(s)}_{O\&M,RES,i}$	[$/kW]	8.84–21.68	8.84–21.68	8.84–21.68	
Alkaline Electrolyzer	$C^{(s)}_{INV,ELY,i}$	[$/kW]	400–850	400–850	400–850	[80]
	$\varsigma_{O\&M,ELY,i}$	[%CAPEX/y]	0.03	0.03	0.03	[80]
	$C^{(s)}_{O\&M,ELY,i}$	[$/kW]	12–25.5	12–25.5	12–25.5	
	$C_{REP,i}$	[$]	120–255	120–255	120–255	
PEM Electrolyzer	$C^{(s)}_{INV,ELY,i}$	[$/kW]	650–1500	650–1500	650–1500	[80]
	$\varsigma_{O\&M,ELY,i}$	[%CAPEX/y]	0.03	0.03	0.03	[80]
	$C^{(s)}_{O\&M,ELY,i}$	[$/kW]	19.5–45	19.5–45	19.5–45	
	$C_{REP,i}$	[$]	195–450	195–450	195–450	[81]
Water[16]	$c^{(s)}_{W}$	[$/m^3]	0.57	0.57	0.57	[82]
Electrical Substation	$C^{(s)}_{INV,SUB,i}$	[$]	49,715	49,715	49,715	[83]
HV/LV equipment	$C^{(s)}_{HV/LV,i}$	[M$]	15	15	15	[84]
Land	$C^{(s)}_{L}$	[$/ha]	5,252	10,504	10,504	Confidential

[16] In 2023 the cost for high consumption user in Tunisia is 1.490 TD/m^3 ≅ 0.50 $/m^3. We increased the cost of about 20 % because of the expected cost increase due to the potential water scarcity.

without applying any structural modification to the pipeline would be equal to 2.6 GSm^3/y. This number is even larger than the maximum volume of hydrogen computed in the three sites, for all the Y years of investment, highlighting how the synthesis of hydrogen would have very little, if no impact on the existing transportation infrastructure.

Table 9 and Table 10 also show the several values of $LCOH_i^{(s)}$ in site 2 and site 3, for every combination of RES and electrolyzer technologies, and also for the different values of their respective investment costs.

In general, the adoption of 1–axis tracker PV plants as the designated RES technology yields slightly lower values of *LCOH* when compared to the fixed–PV alternative, although the specific capital investment for the photovoltaic plants is higher. This implies that the larger CAPEX is offset by the increased hydrogen production.

Considering only the combinations that are feasible in terms of green hydrogen production target and 1–axis tracker PV plants (which proved to be more cost–effective), in site 2 $LCOH_i^{(s)}$ varies between 1.72 $/kg$_{H2}$ and 4.01 $/kg$_{H2}$ in the case of PEM electrolyzers, and between 1.44 $/kg$_{H2}$ and 3.31 $/kg$_{H2}$ with alkaline electrolyzers. In site 3, values lie in the range 1.62 $/kg$_{H2}$ − 3.83 $/kg$_{H2}$ with PEM technology, and in the range 1.34 $/kg$_{H2}$ − 3.17 $/kg$_{H2}$ with the alkaline one.

Fig. 3 and Fig. 4 also show the variation of *LCOH* values for site 2 and site 3 according to the different RES–electrolyzer combinations.

PV-fed plants – Electrolyzer power limit not included

The results shown in the previous section prompt to a meaningful methodological difference between the design approach commonly followed in literature and the one presented in this work. In fact, the first usually follows a power–driven, top–down design, where the size of the renewable plant is obtained from the RES–specific capacity per unit surface, and the overall green hydrogen production multiplying the value of capacity by the specific electricity consumption of the electrolyzer. However, this process does not consider the operating limits of the electrolyzers, namely their activation threshold (lower limit) and overall power capacity (upper limit). As explained in Section 2, hourly values of $p_{h,y}$ that do not lie in the range $\breve{P}_{ELY,j} \leq r_{h,y} \leq P_{ELY,i}$ do not feed the electrolyzers and are injected into the local grid, provided that they do not interfere with the local infrastructural constraints. In other words, computing the production of hydrogen only by means of the specific consumption of the electrolyzers neglects that a certain amount of the electricity generated from renewables could not actually be converted into hydrogen. This is due essentially to the different nature of the electrolyzer input and output: the input is power, the output is energy. Considering the specific consumption of the electrolyzer makes sense only in presence of (enough) constant power, so that also the input to the electrolyzer can be representative, over the time, of an amount of energy that can be completely converted in hydrogen.

Table 6
Numerical results for site 1.

	PV-fixed						*1-axis tracker*					
	$\vartheta = 1$	$\vartheta = 0.9$	$\vartheta = 0.8$	$\vartheta = 0.7$	$\vartheta = 0.6$	$\vartheta = 0.5$	$\vartheta = 1$	$\vartheta = 0.9$	$\vartheta = 0.8$	$\vartheta = 0.7$	$\vartheta = 0.6$	$\vartheta = 0.5$
	PEM Electrolyzer											
$E_{RES}^{(s,i)}$ [GWh]	3173	3525	3966	4533	5288	6346	4064	4515	5079	5805	6773	8127
$E_{ELY}^{(s,i)}$ [GWh]	3173	3525	3966	4500	5008	5487	4064	4515	5079	5732	6212	6588
$E_{grid}^{(s,i)}$ [GWh]	0.00	0.07	0.51	32.32	279.75	858.23	0.01	0.15	0.95	73.25	560.11	1539.59
$M_{H2}^{(s,i)}$ [kt_{H2}]	58.76	65.28	73.44	83.34	92.75	101.62	75.25	83.61	94.05	106.15	115.05	121.99
$V_{H2}^{(s,i)}$ [MNm^3_{H2}]	654	726	817	927	1032	1131	837	930	1046	1181	1280	1357
$W_{H2O}^{(s,i)}$ [kt]	0.98	1.09	1.23	1.39	1.55	1.70	1.26	1.40	1.57	1.77	1.92	2.04
	Alkaline Electrolyzer											
$E_{RES}^{(s,i)}$ [GWh]	3173	3525	3966	4533	5288	6346	4064	4515	5079	5805	6773	8127
$E_{ELY}^{(s,i)}$ [GWh]	3173	3525	3965	4500	5008	5487	4063	4515	5078	5732	6212	6587
$E_{grid}^{(s,i)}$ [GWh]	0.09	0.15	0.59	32.41	279.80	858.28	0.09	0.23	1.02	73.33	560.18	1539.66
$M_{H2}^{(s,i)}$ [kt_{H2}]	57.69	64.09	72.10	81.82	91.06	99.77	73.88	82.09	92.34	104.21	112.95	119.77
$V_{H2}^{(s,i)}$ [MNm^3_{H2}]	642	713	802	910	1013	1110	822	913	1027	1159	1257	1333
$W_{H2O}^{(s,i)}$ [kt]	0.96	1.07	1.20	1.37	1.52	1.67	1.23	1.37	1.54	1.74	1.89	2.00

Table 7
Numerical results for site 2.

	PV-fixed						*1-axis tracker*					
	$\vartheta = 1$	$\vartheta = 0.9$	$\vartheta = 0.8$	$\vartheta = 0.7$	$\vartheta = 0.6$	$\vartheta = 0.5$	$\vartheta = 1$	$\vartheta = 0.9$	$\vartheta = 0.8$	$\vartheta = 0.7$	$\vartheta = 0.6$	$\vartheta = 0.5$
	PEM Electrolyzer											
$E_{RES}^{(s,i)}$ [GWh]	3214	3571	4017	4591	5356	6427	4106	4562	5133	5866	6843	8212
$E_{ELY}^{(s,i)}$ [GWh]	3213	3570	4016	4562	5076	5549	4106	4562	5131	5798	6282	6646
$E_{grid}^{(s,i)}$ [GWh]	0.00	0.13	0.67	28.66	280.33	878.09	0.02	0.24	1.31	67.27	561.41	1565.98
$M_{H2}^{(s,i)}$ [kt_{H2}]	59.51	66.12	74.37	84.48	93.99	102.76	76.04	84.48	95.02	107.38	116.33	123.07
$V_{H2}^{(s,i)}$ [MNm^3_{H2}]	662	736	827	940	1046	1143	846	940	1057	1195	1294	1369
$W_{H2O}^{(s,i)}$ [kt]	0.99	1.10	1.24	1.41	1.57	1.71	1.27	1.41	1.59	1.79	1.94	2.05
	Alkaline Electrolyzer											
$E_{RES}^{(s,i)}$ [GWh]	3214	3571	4017	4591	5356	6427	4106	4562	5133	5866	6843	8212
$E_{ELY}^{(s,i)}$ [GWh]	3213	3570	4016	4562	5075	5549	4106	4562	5131	5798	6282	6646
$E_{grid}^{(s,i)}$ [GWh]	0.07	0.19	0.74	28.73	280.38	878.15	0.08	0.30	1.36	67.34	561.47	1566.04
$M_{H2}^{(s,i)}$ [kt_{H2}]	58.43	64.92	73.02	82.95	92.28	100.89	74.65	82.94	93.29	105.43	114.22	120.84
$V_{H2}^{(s,i)}$ [MNm^3_{H2}]	650	722	812	923	1027	1122	831	923	1038	1173	1271	1344
$W_{H2O}^{(s,i)}$ [kt]	0.98	1.08	1.22	1.38	1.54	1.68	1.25	1.38	1.56	1.76	1.91	2.02

When accounting for the operational features of the electrolyzers, it is possible to infer that maximizing size of the RES plant is not always the most convenient choice, as the increase in RES power capacity is not matched by a proportionate growth in the production of green hydrogen. To this purpose, Table 11 shows the electricity and green hydrogen production in the three sites, in case the size of the PV plant corresponds to the maximum that could be installed, net of the necessary space to install the electrolyzers and the substation, without considering any grid constraint. The table also shows the ratio between the "unconstrained" capacity and the maximum that could be installed complying with all the constraint (as presented in Table 6, Table 7, and Table 8), as well as the ration between their corresponding hydrogen production. It also provides the percentage of renewable electricity that is converted into green hydrogen.

In site 2, although the maximum allowable size of the PV plant – in the case of PV–fixed – is 1.70 times larger than that of the sensitivity analysis, the increase in hydrogen production is only 1.18 times, for any kind of electrolyzer technology. In terms of the exploitation of the electricity produced from renewables, only 57.7% is supplied to the electrolysis plant, whereas in the case of a 200 MW PV plant 86.3% of generated electricity could be converted into hydrogen. A similar trend characterizes 1–axis tracker plants: in fact, despite an oversizing ratio of 1.13, the green hydrogen production is almost the same, as they stand in a 1.03 ratio, and only 73.5% of renewable electricity goes into the

Table 8
Numerical results for Site 3.

	PV-fixed						*1-axis tracker*					
	$\vartheta = 1$	$\vartheta = 0.9$	$\vartheta = 0.8$	$\vartheta = 0.7$	$\vartheta = 0.6$	$\vartheta = 0.5$	$\vartheta = 1$	$\vartheta = 0.9$	$\vartheta = 0.8$	$\vartheta = 0.7$	$\vartheta = 0.6$	$\vartheta = 0.5$
	PEM Electrolyzer											
$E_{RES}^{(s,i)}$ [GWh]	3501	3890	4376	5001	5835	7002	4476	4973	5595	6394	7460	8952
$E_{ELY}^{(s,i)}$ [GWh]	3501	3889	4372	4926	5406	5846	4476	4972	5586	6228	6635	6944
$E_{grid}^{(s,i)}$ [GWh]	0.00	1.14	4.50	75.49	428.65	1156.18	0.02	1.46	8.83	165.93	824.63	2007.67
$M_{H2}^{(s,i)}$ [kt_{H2}]	64.83	72.02	80.96	91.22	100.12	108.26	82.89	92.07	103.45	115.34	122.88	128.60
$V_{H2}^{(s,i)}$ [MNm^3_{H2}]	721	801	901	1015	1114	1204	922	1024	1151	1283	1367	1431
$W_{H2O}^{(s,i)}$ [kt]	1.08	1.20	1.35	1.52	1.67	1.81	1.38	1.54	1.73	1.92	2.05	2.15
	Alkaline Electrolyzer											
$E_{RES}^{(s,i)}$ [GWh]	3501	3890	4376	5001	5835	7002	4476	4973	5595	6394	7460	8952
$E_{ELY}^{(s,i)}$ [GWh]	3501	3889	4372	4926	5406	5846	4476	4972	5586	6228	6635	6944
$E_{grid}^{(s,i)}$ [GWh]	0.11	1.25	4.60	75.59	428.71	1156.25	0.11	1.55	8.93	166.04	824.70	2007.76
$M_{H2}^{(s,i)}$ [kt_{H2}]	63.65	70.70	79.48	89.56	98.30	106.29	81.38	90.39	101.56	113.24	120.64	126.26
$V_{H2}^{(s,i)}$ [MNm^3_{H2}]	708	787	884	996	1094	1183	905	1006	1130	1260	1342	1405
$W_{H2O}^{(s,i)}$ [kt]	1.06	1.18	1.33	1.49	1.64	1.77	1.36	1.51	1.70	1.89	2.01	2.11

Table 9
$LCOH_i^{(s)}$ values (in \$/kg_{H_2}) in site 2.

ϑ	**PEM electrolyzer**								**Alkaline electrolyzer**							
	PV-Fixed				**1-axis tracker**				**PV-Fixed**				**1-axis tracker**			
	$C_{INV,RES,i}^{(s)}$ **Max**		$C_{INV,RES,i}^{(s)}$ **Min**		$C_{INV,RES,i}^{(s)}$ **Max**		$C_{INV,RES,i}^{(s)}$ **Min**		$C_{INV,RES,i}^{(s)}$ **Max**		$C_{INV,RES,i}^{(s)}$ **Min**		$C_{INV,RES,i}^{(s)}$ **Max**		$C_{INV,RES,i}^{(s)}$ **Min**	
	$C_{INV,ELY,i}^{(s)}$				$C_{INV,ELY,i}^{(s)}$				$C_{INV,ELY,i}^{(s)}$				$C_{INV,ELY,i}^{(s)}$			
	Max	**Min**	**Max**	**Min**	**Max**	**Min**	**Max**	**Min**	**Max**	**Min**	**Max**	**Min**	**Max**	**Min**	**Min**	**Max**
1	5.47	3.42	4.55	2.51	4.78	3.18	3.77	2.17	3.97	2.87	3.04	1.94	3.62	2.59	2.59	1.73
0.9	5.07	3.23	4.16	2.32	4.47	3.03	3.46	2.02	3.73	2.74	2.80	1.81	3.43	2.40	2.40	1.62
0.8	4.68	3.04	3.77	2.13	4.16	2.88	3.15	1.87	3.49	2.61	2.56	1.68	3.24	2.21	2.21	1.52
0.7	4.31	2.87	3.40	1.95	3.90	2.77	2.88	1.74	3.27	2.49	2.34	1.56	3.09	2.05	2.05	1.44
0.6	4.11	2.81	3.15	1.85	3.87	2.82	2.77	1.72	3.18	2.48	2.20	1.50	3.12	2.00	2.00	1.44
0.5	4.06	2.87	3.00	1.81	4.01	3.02	2.76	1.77	3.21	2.57	2.13	1.49	3.31	2.04	2.04	1.50

electrolyzers, compared against 80.9% of the 200 MW plant.

Such values corroborate the fact that significantly increasing the size of the renewable plant does not yield as large values, in terms of green hydrogen production.

The pre–feasibility study also included the assessment of electricity production from wind generators. However, due to the limited land availability in the three sites, coupled with the considerably larger surface requirements of wind farms when compared to PV [73] the solution was discarded at the early stages of the analysis. Additionally, the only location that would have been suitable to accommodate a wind generation power plant was site 1, i.e., the only one characterized by high enough wind speeds. Considering the technical features of the wind generators presented in Table 3, only three turbines could be installed in site 1, for an overall capacity of just 12 MW.

For sake of completeness, Table 12 shows the numerical results obtained considering electricity generation from wind in site 1, for the two considered electrolyzer technologies, and for rotor hub heights of 105 m and 166 m.

Table 13 also shows the values of in the case of electricity production from wind turbines.

The selection of wind turbines yields a considerably larger *LCOH*, due to both its larger specific capital cost, and the limited amount of green hydrogen that could be produced, in light of the modest overall installable capacity. In the case of a rotor hub height of 105 m, $LCOH_i^{(s)}$ varies between 5.46 \$/kg_{H2} and 11.09 \$/kg_{H2} in the case of PEM electrolyzers, and between 5.34 \$/kg_{H2} and 9.94 \$/kg_{H2} with alkaline electrolyzers. Taller towers grant slightly lower levelized costs, thanks to the opportunity of harnessing higher windspeeds and consequently of generating more electricity and green hydrogen.

Discussion

Complementing the presentation of the numerical results of the study, it is worth wrapping the analysis with some additional comments, regarding how the development of a green hydrogen supply chain in Tunisia would impact its energy system. In fact, although the country benefits from weather conditions that are very favorable to the

Table 10
$LCOH_1^{(s)}$ values (in \$/kg$_{H_2}$) in site 3.

ϑ	PEM electrolyzer								Alkaline electrolyzer							
	PV-Fixed				1-axis tracker				PV-Fixed				1-axis tracker			
	$C_{INV,RES,i}^{(s)}$ Max		$C_{INV,RES,i}^{(s)}$ Min		$C_{INV,RES,i}^{(s)}$ Max		$C_{INV,RES,i}^{(s)}$ Min		$C_{INV,RES,i}^{(s)}$ Max		$C_{INV,RES,i}^{(s)}$ Min		$C_{INV,RES,i}^{(s)}$ Max		$C_{INV,RES,i}^{(s)}$ Min	
	$C_{INV,ELY,i}^{(s)}$				$C_{INV,ELY,i}^{(s)}$				$C_{INV,ELY,i}^{(s)}$				$C_{INV,ELY,i}^{(s)}$			
	Max	Min	Max	Min	Max	Min	Max	Min	Max	Min	Max	Min	Max	Min	Max	Min
1	5.02	3.14	4.18	2.30	4.38	2.91	3.46	1.99	3.64	2.63	2.79	1.78	3.32	2.53	2.37	1.58
0.9	4.66	2.96	3.82	2.13	4.10	2.78	3.17	1.85	3.42	2.51	2.57	1.66	3.15	2.43	2.20	1.49
0.8	4.30	2.79	3.46	1.96	3.82	2.65	2.90	1.72	3.21	2.39	2.35	1.54	2.98	2.34	2.03	1.40
0.7	3.99	2.66	3.15	1.81	3.63	2.57	2.68	1.62	3.03	2.31	2.16	1.44	2.88	2.31	1.91	1.34
0.6	3.86	2.64	2.95	1.74	3.66	2.67	2.62	1.63	2.98	2.32	2.06	1.41	2.96	2.42	1.89	1.36
0.5	3.85	2.72	2.85	1.72	3.83	2.89	2.64	1.69	3.04	2.44	2.02	1.42	3.17	2.66	1.95	1.44

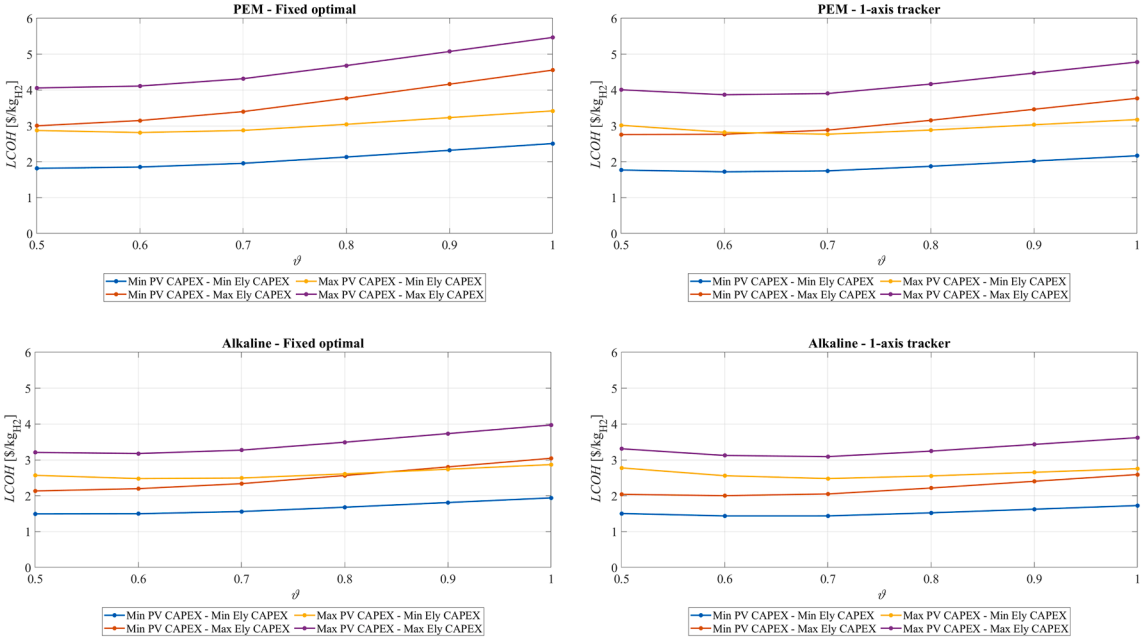

Fig. 3. Site 2.

penetration of renewable sources, the first potential obstacle to the commercial scale penetration of green hydrogen is that Tunisia can count on limited freshwater resources. Hence, the idea of withdrawing freshwater locally for electrolysis is unlikely, given that, as per in 2020, freshwater withdrawals in Tunisia accounted for 98.1% of the total local freshwater resources [86]. Therefore, the Tunisian Ministry of Industry, Mines and Energy is currently planning to implement its green hydrogen strategy leaving the national freshwater resources intact, and resorting to seawater desalination to meet the electrolyzers needs. Thanks to its negligible additional cost – estimated at about 0.01–0.02 \$/kg$_{H2}$ – to be added on top of the overall hydrogen production, desalination was designated as the technology devoted to producing freshwater for electrolysis. According to governmental estimates, in 2030 the Tunisian seawater needs for desalination purposes, compared with a green hydrogen production target of about 320 kt$_{H2}$/y, should be between 6.4–9.6 Mm^3/y [46].

Regardless the commitment of the Tunisian government to overcome the barriers imposed by the absence of freshwater, the efforts foreseen by Tunisia in its green hydrogen strategy are undoubtedly ambitious: 3.85 GW of electrolyzer capacity should already be deployed by 2030, compared against just 510 GW of total renewable installed capacity at the end of 2022 [33]. Financially, overall investments in the period 2025–2030 were estimated at 117 B€ (approximately 128 B\$), which is about two orders of magnitude larger with respect to what Tunisia had invested in the period 2001–2021 in renewable energies, i.e., approximately 1 B\$ [33].

Nevertheless, the Tunisian government may be ready to trade off such an outstanding effort with returns on multiple sides. First, the development of a green hydrogen supply chain in Tunisia will naturally be beneficial from the environmental point of view, achieving GHG savings as large as about 217 kt$_{CO2eq}$/y in 2030, and up to 19,000 kt$_{CO2eq}$/y in 2050.

Hydrogen penetration in the national energy mix would also be capable of creating around 19,000 new job vacancies in 2030 and, at the same time, bring considerable amounts of money into the Tunisian economy, considering that most of the hydrogen is destined to be exported. As such, revenues coming from the export of green hydrogen and its derived products could be equal to 2.35 B\$ in 2035 and be as high as 9.4 B\$ in 2050 [46].

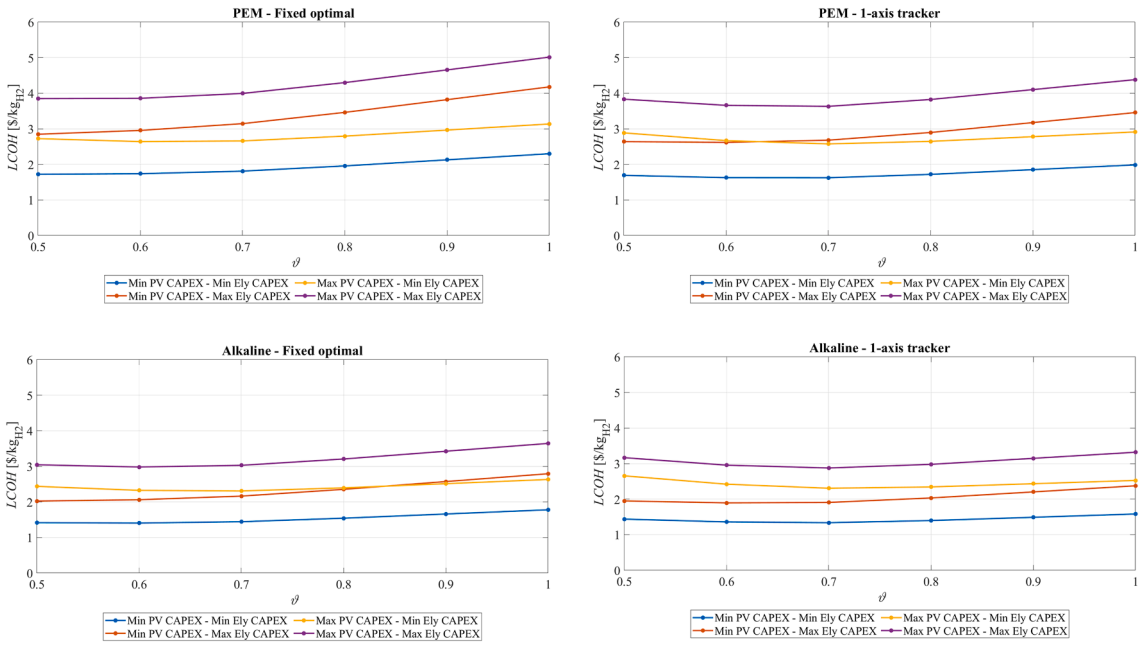

Fig. 4. Site 3.

Table 11
Comparison between the results of the sensitivity analysis and those obtained with the maximum PV capacity.

		PV–fixed		1–axis Tracker	
		PEM	ALK	PEM	ALK
Site 1	$P_{RES}^{(s,i)}$ [MW]	140.0	139.9	93.4	93.3
	$P_{RES}^{(s,i)}/P_{RES,max}^{(s,i)}$	1.26	1.12		
	$E_{RES}^{(s,i)}$ [GWh]	4443	4439	3794	3790
	$E_{ELY}^{(s,i)}$ [GWh]	4423	4420	3794	3790
	$E_{grid}^{(s,i)}$ [GWh]	20.03	19.66	0.02	0.09
	$E_{ELY}^{(s,i)}/E_{RES}^{(s,i)}$	99.5%	99.6%	99.9%	99.9%
	$M_{H2}^{(s,i)}$ [kt$_{H2}$]	81.91	80.36	70.26	68.91
	$M_{H2}^{(s,i)}/M_{H2,max}^{(s,i)}$	1.25	1.11		
Site 2	$P_{RES}^{(s,i)}$ [MW]	340.0	339.9	226.7	226.6
	$P_{RES}^{(s,i)}/P_{RES,max}^{(s,i)}$	1.70	1.70	1.13	1.13
	$E_{RES}^{(s,i)}$ [GWh]	10,927	10,923	9308	9305
	$E_{ELY}^{(s,i)}$ [GWh]	6522	6521	6842	6841
	$E_{grid}^{(s,i)}$ [GWh]	4406	4402	2466	2463
	$E_{ELY}^{(s,i)}/E_{RES}^{(s,i)}$	59.7%	59.7%	73.5%	73.5%
	$M_{H2}^{(s,i)}$ [kt$_{H2}$]	120.77	118.56	126.70	124.39
	$M_{H2}^{(s,i)}/M_{H2,max}^{(s,i)}$	1.18	1.18	1.03	1.03
Site 3	$P_{RES}^{(s,i)}$ [MW]	331.0	220.7	330.9	220.6
	$P_{RES}^{(s,i)}/P_{RES,max}^{(s,i)}$	1.66	1.65	1.10	1.10
	$E_{RES}^{(s,i)}$ [GWh]	11,590	11,585	9878	9874
	$E_{ELY}^{(s,i)}$ [GWh]	6693	6693	7078	7077
	$E_{grid}^{(s,i)}$	4897	4893	2800	2797
	$E_{ELY}^{(s,i)}/E_{RES}^{(s,i)}$	57.7%	57.8%	71.7%	71.7%
	$M_{H2}^{(s,i)}$ [kt$_{H2}$]	123.95	121.68	131.07	128.68
	$M_{H2}^{(s,i)}/M_{H2,max}^{(s,i)}$	1.14	1.14	1.02	1.02

Table 12
Numerical results for site 1, in the case of generation from WT.

	Rotor hub height: 105 m	Rotor hub height: 166 m
	PEM Electrolyzer	
$E_{RES}^{(s,i)}$ [GWh]	1358	1400
$E_{ELY}^{(s,i)}$ [GWh]	1358	1400
$E_{grid}^{(s,i)}$ [GWh]	0.18	0.16
$M_{H2}^{(s,i)}$ [Mt$_{H2}$]	25.15	25.93
$V_{H2}^{(s,i)}$ [MNm^3$_{H2}$]	279.85	288.47
$W_{H2O}^{(s,i)}$ [Mm^3]	0.42	0.43
	Alkaline Electrolyzer	
$E_{RES}^{(s,i)}$ [GWh]	1358	1400
$E_{ELY}^{(s,i)}$ [GWh]	1357	1399
$E_{grid}^{(s,i)}$ [GWh]	1.22	1.09
$M_{H2}^{(s,i)}$ [Mt$_{H2}$]	24.68	25.44
$V_{H2}^{(s,i)}$ [MNm^3$_{H2}$]	274.55	283.03
$W_{H2O}^{(s,i)}$ [Mm^3]	0.41	0.42

Concluding remarks

In this paper, we investigated the potential role of renewables and green hydrogen in the Mediterranean basin, with reference to three specific production sites located in Tunisia. The proposed feasibility study was commissioned with the aim of assessing the potentiality of delivering green hydrogen to Italy, by blending it with natural gas in the Transmed gas pipeline.

The idea was prompted by considering that the total transport capacities of the Southern–Northern Mediterranean natural gas interconnectors are currently underexploited, with respect to their design values. Therefore, there could be the chance of blending green hydrogen with natural gas and, in perspective, integrating it into the energy mixes of Mediterranean countries, progressively shifting from a black to a green energy dialogue across the three shores using existing pipelines from the South building new ones connecting the Eastern and Northern shores, as long as the political and security conditions in the area will allow it, in addition to the Trans Adriatic Pipeline (TAP) from Azerbaijan.

Furthermore, such long–term perspective would prevent the existing natural gas transport infrastructure from being dismissed and ultimately phased–out, while simultaneously offering the countries of the Southern

Table 13
$LCOH_i^{(s)}$ values in site 1 in the case of wind electricity generation.

PEM electrolyzer								Alkaline electrolyzer							
105 m				166 m				105 m				166 m			
$C_{INV,RES,i}^{(s)}$		$C_{INV,RES,i}^{(s)}$		$C_{INV,RES,i}^{(s)}$		$C_{INV,RES,i}^{(s)}$		$C_{INV,RES,i}^{(s)}$		$C_{INV,RES,i}^{(s)}$		$C_{INV,RES,i}^{(s)}$		$C_{INV,RES,i}^{(s)}$	
Max		**Min**		**Max**		**Min**		**Max**		**Min**		**Max**		**Min**	
$C_{INV,ELY,i}^{(s)}$				$C_{INV,ELY,i}^{(s)}$				$C_{INV,ELY,i}^{(s)}$				$C_{INV,ELY,i}^{(s)}$			
Max	**Min**	**Max**	**Min**	**Max**	**Min**	**Max**	**Min**	**Max**	**Min**	**Max**	**Min**	**Max**	**Min**	**Max**	**Min**
11.09	6.24	10.31	5.46	9.94	5.34	9.94	5.34	7.52	4.91	6.73	4.12	5.41	2.87	5.41	2.87

shore the opportunity to diversify their sources of income, which for some of them are presently mostly coming from the export of fossil fuels.

Paradoxically, the current black dialogue originates from the South shore, which is the most promising in terms of sun and wind resources (with an average global horizontal irradiance of 5.67 kWh/m^2 and an average wind speed of 8.76 m/s, both larger than their Eastern shore and Northern shore counterparts). Conversely, the main portion of the Mediterranean energy demand is split between the Northern and Eastern shores. For this reason, fostering the capillary diffusion of RES in the Southern shore would help accomplishing its decarbonization, as well as the development of renewed Mediterranean energy system, characterized by the production and trade of renewable electricity and green hydrogen.

Such a complex and multifaceted process must be supported by robust and reliable preliminary analyses, aiming at quantifying the electricity and green hydrogen producibility potential in specific locations of the Southern shore. In this paper we proved that, in order to be consistent, mathematical models devoted to the evaluation of renewable electricity and green hydrogen generation should not only consider weather data (regardless how fine they could be), but also and more importantly the geographical and infrastructural constraints, to not overestimate the amount of available electricity.

Moreover, we showed that multiplying the renewable electricity generation by the efficiency and/or specific consumption of the electrolyzers overestimates the production of green hydrogen, because the operating thresholds of the electrolyzers are not accounted for. Consequently, such approaches wrongly assume that 100% of the electricity feeding the electrolyzers can be converted into green hydrogen, whereas some is actually curtailed, wasted, or injected into the local distribution grid, as considered in this work. For example, the electricity diverted to the local grid could be as large as 19.0% and 22.5% of the total PV generation, in the case of a 1–axis tracker plant, for site 2 and site 3, respectively.

Secondarily, we proved that – keeping the size of the electrolysis plant fixed – increasing the capacity of the RES plant does not necessarily imply a proportionate increase in the amount of produced green hydrogen, as larger amounts of electricity will be sent to the distribution grid instead of feeding the electrolysis group. In the case of fixed–PV plant, increasing the RES capacity of 70% in site 2 only yielded a 18% increase in green hydrogen production. Similarly, in site 3, oversizing the photovoltaic plant by approximately 65% produced only a 14% gain in terms of synthetized green hydrogen.

In site 2, *LCOH* varied between 1.49 \$/kg$_{H2}$ and 4.06 \$/kg$_{H2}$ and between 1.77 \$/kg$_{H2}$ and 4.01 \$/kg$_{H2}$, for a 200 MW PV–fixed and 1–axis tracker plant, respectively. The corresponding combinations for site 3 provide a range of 1.42 \$/kg$_{H2}$-3.85 \$/kg$_{H2}$ for PV–fixed plants, and of 1.44 \$/kg$_{H2}$ and 3.83 \$/kg$_{H2}$ for 1–tracker plants.

In perspective, the sensitivity analysis presented in this study could be further enhanced by developing a mathematical optimization that could enable the simultaneous integration of several RES and electrolyzer technologies and models, and the definition of the plant layout that best fits the local topological constraints – hence matching the necessary green hydrogen production – while trading it off with reasonable overall capital and operational expenditures. This more exhaustive computational approach will be investigated in future works.

CRediT authorship contribution statement

A. Mazza: Writing – review & editing, Writing – original draft, Supervision, Methodology, Investigation, Formal analysis, Conceptualization. **A. Forte:** Writing – review & editing, Writing – original draft, Software, Investigation, Formal analysis, Data curation. **E. Bompard:** Visualization, Validation, Resources, Funding acquisition. **G. Cavina:** Validation, Project administration, Data curation. **A.M. Angelini:** Visualization, Validation, Project administration. **M. Melani:** Writing – review & editing, Resources, Funding acquisition.

Declaration of competing interest

The authors declare that they have no known competing financial interests or personal relationships that could have appeared to influence the work reported in this paper.

Data availability

The data that has been used is confidential.

Acknowledgments

The authors would like to thank Imed Derouiche from H2G (Tunisia) for having provided some of the data used in this study.

Appendix A. Supplementary data

Supplementary data to this article can be found online at https://doi.org/10.1016/j.ecmx.2024.100614.

References

[1] Unfcc. COP27: Delivering for people and the planet. United Nations; 2022.
[2] UNFCC. (2023). *COP28 UAE - United Nations Climate Change Conference*. https://www.cop28.com/en/.
[3] ClimateWatch. (2019). *GHG Emissions*. https://www.climatewatchdata.org/.
[4] Our World in Data. (2022). *Carbon intensity of electricity*. https://ourworldindata.org/grapher/carbon-intensity-electricity.
[5] European Parliament, & European Council. (2018). Directive (EU) 2018/2001 of the European Parliament and of the Council of 11 December 2018 on the promotion of the use of energy from renewable sources (recast). https://eur-lex.europa.eu/eli/dir/2018/2001/oj.
[6] Bartels J, Varela C, Wassermann T, Medjroubi W, Zondervan E. Integration of water electrolysis facilities in power grids: a case study in northern Germany. Energy Convers Manage: X 2022;14:100209. https://doi.org/10.1016/J.ECMX.2022.100209.
[7] Bhaskar A, Assadi M, Somehsaraei HN. Can methane pyrolysis based hydrogen production lead to the decarbonisation of iron and steel industry? Energy Convers Manage: X 2021;10:100079. https://doi.org/10.1016/J.ECMX.2021.100079.
[8] Zier M, Pflugradt N, Stenzel P, Kotzur L, Stolten D. Industrial decarbonization pathways: the example of the German glass industry. Energy Convers Manage: X 2023;17:100336. https://doi.org/10.1016/J.ECMX.2022.100336.

[9] IRENA. (2022). *Green Hydrogen for Industry: A Guide to Policy Making*. https://irena.org/publications/2022/Mar/Green-Hydrogen-for-Industry.

[10] Bailey C, & al. (1999). The Green Hydrogen Report - The 1995 Progress Report of the Secretary of Energy's Hydrogen Technical Advisory Panel.

[11] Velazquez Abad A, Dodds PE. Green hydrogen characterisation initiatives: definitions, standards, guarantees of origin, and challenges. Energy Policy 2020; 138:111300. https://doi.org/10.1016/J.ENPOL.2020.111300.

[12] Mazza A, Salomone F, Arrigo F, Bensaid S, Bompard E, Chicco G. Impact of Power-to-Gas on distribution systems with large renewable energy penetration. Energy Convers Manage: X 2020;7. https://doi.org/10.1016/J.ECMX.2020.100053.

[13] CHN Energy. (2021). *China Hydrogen Alliance Unveils the World's First 'Green Hydrogen' Standard*. https://www.ceic.com/gjnyjtwwEn/xwzx/202101/e9147965a7e5465d8d3419fafdfa2355.shtml.

[14] Clean Hydrogen Production Standard Guidance : DOE Hydrogen Program. 2022. https://www.hydrogen.energy.gov/clean-hydrogen-production-standard.html.

[15] Hydrogen Council. (2021). *Hydrogen decarbonization pathways A life-cycle assessment*. www.hydrogencouncil.com.

[16] World Bank. (2024). *Open Data*. https://data.worldbank.org/.

[17] Worldbank. (2024). *Worldwide Governance Indicators*. http://info.worldbank.org/governance/wgi/.

[18] IEA. (2024). *Energy Statistics Data Browser*. https://www.iea.org/data-and-statistics/data-tools/energy-statistics-data-browser?country=FRANCE&fuel=Energy%20supply&indicator=TESbySource.

[19] IRENA. (2023a). *IRENASTAT Online Data Query Tool*. https://pxweb.irena.org/pxweb/en/IRENASTAT?_gl=1*1mjq85n*_ga*MTAxMTU4NDY5Ny4xNjU1MTI4MTg2*_ga_7W6ZEF19K4*MTY2NTA3MzI4My4xMy4wLjE2NjUwNzMyODMuNjAuMC4w.

[20] Norouzi N. Assessment of technological path of hydrogen energy industry development: a review. Iran J Energy Environ 2021;12(4):273–84. https://doi.org/10.5829/IJEE.2021.12.04.01.

[21] British Petroleum. Statistical Review of World Energy. 2023. https://www.bp.com/en/global/corporate/energy-economics/statistical-review-of-world-energy.html.

[22] Eurostat. Imports of natural gas by partner country. 2022. https://ec.europa.eu/eurostat/databrowser/view/nrg_ti_gas/default/table?lang=en&category=nrg.nrg_quant.nrg_quanta.nrg_t.nrg_ti.

[23] Eurostat. Imports of oil and petroleum products by partner country. https://ec.europa.eu/eurostat/databrowser/product/view/nrg_ti_oil?category=nrg.nrg_quant.nrg_quanta.nrg_t.nrg_ti.

[24] Enagás. (2023a). *Gas Statistical Bulletin*. https://www.enagas.es/en/technical-management-system/energy-data/publications/gas-statistical-bulletin/.

[25] Snam. (2022). *Dati operativi business*. https://www.snam.it/it/trasporto/dati-operativi-business/.

[26] AXSMarine. (2023). *Alphatanker*. https://public.axsmarine.com/alphatanker.

[27] Country Profiles. The Observatory of Economic Complexity (OEC). 2021. https://oec.world/en.

[28] European Commission. (2018). *2050 long-term strategy*. https://climate.ec.europa.eu/eu-action/climate-strategies-targets/2050-long-term-strategy_en.

[29] European Commission. (2020b). *The European Green Deal*. https://www.europarl.europa.eu/doceo/document/TA-9-2020-0005_EN.html.

[30] Our World in Data. *CO_2 and Greenhouse Gas Emissions Data Explorer*; 2021. https://ourworldindata.org/explorers/co2?time=latest&facet=none&country=~OWID_EU27&Gas+or+Warming=All+GHGs+%28CO%E2%82%82eq%29&Accounting=Production-based&Fuel+or+Land+Use+Change=All+fossil+emissions&Count=Per+country&Relative+to+world+total=true.

[31] Solargis s.r.o. (2022). *Global Solar Atlas*.

[32] Technical University of Denmark (DTU), & World Bank Group. (2022). *Global Wind Atlas*.

[33] IRENA. (2023b). *IRENASTAT Online Data Query Tool*. https://www.irena.org/Data/Downloads/IRENASTAT.

[34] Noussan M, Raimondi PP, Scita R, Hafner M. (2021). The role of green and blue hydrogen in the energy transition—a technological and geopolitical perspective. In *Sustainability (Switzerland)* (Vol. 13, Issue 1, pp. 1–26). MDPI AG. https://doi.org/10.3390/su13010298.

[35] Scita R, Raimondi PP, Noussan M. Green hydrogen: The holy grail of decarbonisation? An analysis of the technical and geopolitical implications of the future hydrogen economy. SSRN Electron J 2020. https://doi.org/10.2139/SSRN.3709789.

[36] van Wijk A, Wouters F. Hydrogen-the bridge between Africa and Europe. Shap Inclusive Energy Transit 2021;91–119. https://doi.org/10.1007/978-3-030-74586-8_5/TABLES/7.

[37] European Commission. (2020a). *A hydrogen strategy for a climate-neutral Europe*. https://eur-lex.europa.eu/legal-content/EN/TXT/?uri=CELEX:52020DC0301.

[38] Ministry of Economy and Sustainable Development. *Hydrogen Strategy of the Republic of Croatia unitil 2050*; 2022. https://mingor.gov.hr/UserDocsImages/UPRAVA%20ZA%20ENERGETIKU/Croatian%20Hydrogen%20Strategy%20ENG%20FIN%2022%208.pdf.

[39] European Commission. (2023a). *France - Draft Updated NECP 2021-2030*. https://commission.europa.eu/publications/france-draft-updated-necp-2021-2030_en.

[40] Οικονομικός Ταχυδρόμος. (2023). *Greek Hydrogen Strategy: Domestic production of 3,500 GWh in 2030*. https://www.ot.gr/2022/06/07/english-edition/greek-hydrogen-strategy-domestic-production-of-3500-gwh-in-2030/.

[41] European Commission. (2023b). *Italy - Draft Updated NECP 2021-2030* . https://commission.europa.eu/publications/italy-draft-updated-necp-2021-2030_en.

[42] European Commission. (2023c). *Portugal - Draft Updated NECP 2021-2030* . https://commission.europa.eu/publications/portugal-draft-updated-necp-2021-2030_en.

[43] European Commission. (2023d). *Slovenia - Draft Updated NECP 2021-2030*. https://commission.europa.eu/publications/slovenia-draft-updated-necp-2021-2030_en.

[44] European Commission. (2023e). *Spain - Draft Updated NECP 2021-2030*. https://commission.europa.eu/publications/spain-draft-updated-necp-2021-2030_en.

[45] Royaume du Maroc. (2021). *Feuille de route. Hydrogène vert. Vecteur de Transition Énergétique et de Croissance Durable*. https://www.mem.gov.ma/Lists/Lst_rapports/Attachments/36/Feuille%20de%20route%20de%20hydrog%C3%A8ne%20vert.pdf.

[46] giz, & Ministére de l'Industrie, des M. et de l'Energie. (2023). *L'hydrogène vert pour un développement économique durable et une économie décarbonisée en Stratégie nationale pour le développement de l'hydrogène vert et ses dérivés en Tunisie*.

[47] République Algérienne Démocratique et Populaire. (2023). *Stratégie Nationale de Développement de l'Hydrogen en Algérie*.

[48] Egypt Oil & Gas. (2023, November 23). *National Green Hydrogen Council Approves Green Hydrogen Strategy*. https://egyptoil-gas.com/news/national-green-hydrogen-council-approves-green-hydrogen-strategy/.

[49] STIP Compass. (2023). *TÜRKİYE HYDROGEN TECHNOLOGIES STRATEGY AND ROADMAP*. https://stip.oecd.org/stip/interactive-dashboards/policy-initiatives/2023%2Fdata%2FpolicyInitiatives%2F99992395.

[50] European Hydrogen Backbone. (2022). *A EUROPEAN HYDROGEN INFRASTRUCTURE VISION COVERING 28 COUNTRIES*. https://www.ehb.eu/maps.

[51] Gaugl R, Bachhiesl U. Potentials and systemic aspects for the integration of renewable energies in the North African and Middle Eastern electricity system. Elektrotechnik Und Informationstechnik 2020;137(8):487–94. https://doi.org/10.1007/s00502-020-00848-z.

[52] Rahmouni S, Negrou B, Settou N, Dominguez J, Gouareh A. Prospects of hydrogen production potential from renewable resources in Algeria. Int J Hydrogen Energy 2017;42(2):1383–95. https://doi.org/10.1016/j.ijhydene.2016.07.214.

[53] Rahmouni S, Settou N, Negrou B, Chennouf N, Ghedamsi R. (2015). Prospects and analysis of hydrogen production from renewable electricity sources in algeria. In *Progress in Clean Energy, Volume 2: Novel Systems and Applications* (pp. 583–602). Springer International Publishing. https://doi.org/10.1007/978-3-319-17031-2_42.

[54] Abdin Z, Mérida W. Hybrid energy systems for off-grid power supply and hydrogen production based on renewable energy: a techno-economic analysis. Energy Convers Manage 2019;196:1068–79. https://doi.org/10.1016/J.ENCONMAN.2019.06.068.

[55] Al-Sharafi A, Sahin AZ, Ayar T, Yilbas BS. Techno-economic analysis and optimization of solar and wind energy systems for power generation and hydrogen production in Saudi Arabia. Renew Sustain Energy Rev 2017;69:33–49. https://doi.org/10.1016/J.RSER.2016.11.157.

[56] Gu Y, Wang D, Chen Q, Tang Z. Techno-economic analysis of green methanol plant with optimal design of renewable hydrogen production: a case study in China. Int J Hydrogen Energy 2022;47(8):5085–100. https://doi.org/10.1016/j.ijhydene.2021.11.148.

[57] Yates J, Daiyan R, Patterson R, Egan R, Amal R, Ho-Baille A, et al. Techno-economic analysis of hydrogen electrolysis from off-grid stand-alone photovoltaics incorporating uncertainty analysis. Cell Rep Phys Sci 2020;1(10):100209. https://doi.org/10.1016/J.XCRP.2020.100209.

[58] He W, Grant RJ, Baden V, Bo-xi Zhang S, Song P, Deng S-S, Singh G, Lozi J, Guyon O, Woznicki M, Le Solliec G, Loisel R. Far off-shore wind energy-based hydrogen production: technological assessment and market valuation designs. J Phys Conf Ser 2020;1669(1):012004. https://doi.org/10.1088/1742-6596/1669/1/012004.

[59] Touili S, Alami Merrouni A, El Hassouani Y, Amrani A, Rachidi S. Analysis of the yield and production cost of large-scale electrolytic hydrogen from different solar technologies and under several Moroccan climate zones. Int J Hydrogen Energy 2020;45(51):26785–99. https://doi.org/10.1016/j.ijhydene.2020.07.118.

[60] Berrada A, Laasmi MA. Technical-economic and socio-political assessment of hydrogen production from solar energy. J Storage Mater 2021;44. https://doi.org/10.1016/j.est.2021.103448.

[61] Jovan DJ, Dolanc G, Pregelj B. Utilization of excess water accumulation for green hydrogen production in a run-of-river hydropower plant. Renew Energy 2022;195:780–94. https://doi.org/10.1016/J.RENENE.2022.06.079.

[62] Negrou B, Settou N, Chennouf N, Dokkar B. Valuation and development of the solar hydrogen production. Int J Hydrogen Energy 2011;36(6):4110–6. https://doi.org/10.1016/J.IJHYDENE.2010.09.013.

[63] Guzzini A, Pellegrini M, Saccani C. (2021). *Green hydrogen valleys: a preliminary case study for the industrial area of Ravenna*. https://www.researchgate.net/publication/358694005_Green_hydrogen_valleys_a_preliminary_case_study_for_the_industrial_area_of_Ravenna.

[64] Vidal-Barrero F, Baena-Moreno FM, Preciado-Cárdenas C, Villanueva-Perales Á, Reina TR. Hydrogen production from landfill biogas: Profitability analysis of a real case study. Fuel 2022;324:124438. https://doi.org/10.1016/J.FUEL.2022.124438.

[65] Pellegrini M, Guzzini A, Saccani C. A preliminary assessment of the potential of low percentage green hydrogen blending in the Italian Natural Gas Network. Energies 2020;13(21). https://doi.org/10.3390/en13215570.

[66] Cavana M, Leone P. Solar hydrogen from North Africa to Europe through greenstream: a simulation-based analysis of blending scenarios and production plant sizing. Int J Hydrogen Energy 2021;46(43):22618–37. https://doi.org/10.1016/j.ijhydene.2021.04.065.

[67] Cavana M, Mazza A, Chicco G, Leone P. Electrical and gas networks coupling through hydrogen blending under increasing distributed photovoltaic generation. Appl Energy 2021;290. https://doi.org/10.1016/j.apenergy.2021.116764.

[68] Rahmouni S, Settou N, Negrou B, Gouareh A. GIS-based method for future prospect of hydrogen demand in the Algerian road transport sector. Int J Hydrogen Energy 2016;41(4):2128–43. https://doi.org/10.1016/j.ijhydene.2015.11.156.
[69] Timmerberg S, Kaltschmitt M. Hydrogen from renewables: Supply from North Africa to Central Europe as blend in existing pipelines – Potentials and costs. Appl Energy 2019;237:795–809. https://doi.org/10.1016/j.apenergy.2019.01.030.
[70] Van de Graaf T, Overland I, Scholten D, Westphal K. The new oil? The geopolitics and international governance of hydrogen. Energy Res Soc Sci 2020;70. https://doi.org/10.1016/j.erss.2020.101667.
[71] Politecnico di Torino. (2019). *RES-Plat: Energy planning platform*. https://www.knowledge-share.eu/en/patent/res-plat/.
[72] IEA. (2023). *Solar PV – Analysis*. https://www.iea.org/reports/solar-pv.
[73] Bompard E, Ciocia A, Grosso D, Huang T, Spertino F, Jafari M, et al. Assessing the role of fluctuating renewables in energy transition: methodologies and tools. Appl Energy 2022;314:118968. https://doi.org/10.1016/j.apenergy.2022.118968.
[74] Cummins Inc., (2021), *Water Electrolyzers. HyLYZER 400 & 500 Spec Sheet*. https://www.cummins.com/new-power/applications/about-hydrogen.
[75] Nel Hydrogen. Atmospheric Alkaline Electrolyser. https://nelhydrogen.com/product/atmospheric-alkaline-electrolyser-a-series/.
[76] Sem Masolini. (2023). *Progettazione e Costruzione di cabine elettriche prefabbricate*. https://semmasolini.it/.
[77] IRENA. (2019b). Future of Wind. In *International Renewable Energy Agency (IRENA) is*.
[78] IRENA. (2019a). *Future of Solar Photovoltaic*. www.irena.org/publications.
[79] Talavera DL, Muñoz-Cerón E, Ferrer-Rodríguez JP, Pérez-Higueras PJ. Assessment of cost-competitiveness and profitability of fixed and tracking photovoltaic systems: The case of five specific sites. Renew Energy 2019;134:902–13. https://doi.org/10.1016/J.RENENE.2018.11.091.
[80] IEA. (2019). *The Future of Hydrogen*.
[81] Zampini M, Consoli D, Brunetto P, Prevedello P, Del Vecchio L, Varoli I. (2022). *How to make green hydrogen competitive by 2030 in the hard-to-abate sectors*. https://www.convegni.aeit.it/misw7/struttura/pagedin.php?web=aeit2022&page_cod=conf_paperlist&page_mod=open&sss=TS02&page_exit=conf_stlist.
[82] Guide de l'Investisseur Tunisie. (2023). *Facteurs de production - Eau potable*. https://guide.tia.gov.tn/fr/production_factors.
[83] Chojnacki AL. Optimum in-service time periods of MV/LV transformer–distribution substations. Electr Pow Syst Res 2012;83(1):212–9. https://doi.org/10.1016/J.EPSR.2011.11.010.
[84] PEguru. (2023). *Substation Cost Estimator*. https://peguru.com/substation-cost-estimator/.
[85] marcogaz. (2019). *OVERVIEW OF AVAILABLE TEST RESULTS AND REGULATORY LIMITS FOR HYDROGEN ADMISSION INTO EXISTING NATURAL GAS INFRASTRUCTURE AND END USE*.
[86] United Nations - UN Water. (2020). *SDG 6 Data*. https://sdg6data.org/en/maps.